AEDC-TR-73-169

cy 2

EXPERIMENTAL VERIFICATION OF A TECHNIQUE FOR TESTING FULL-SCALE INLET/ENGINE SYSTEMS AT ANGLES OF ATTACK UP TO 20 DEG AT TRANSONIC SPEEDS

R. L. Palko

ARO, Inc.

October 1973

TECHNICAL REPORTS
FILE COPY

Approved for public release; distribution unlimited.

PROPULSION WIND TUNNEL FACILITY
ARNOLD ENGINEERING DEVELOPMENT CENTER
AIR FORCE SYSTEMS COMMAND
ARNOLD AIR FORCE STATION, TENNESSEE

NOTICES

When U. S. Government drawings specifications, or other data are used for any purpose other than a definitely related Government procurement operation, the Government thereby incurs no responsibility nor any obligation whatsoever, and the fact that the Government may have formulated, furnished, or in any way supplied the said drawings, specifications, or other data, is not to be regarded by implication or otherwise, or in any manner licensing the holder or any other person or corporation, or conveying any rights or permission to manufacture, use, or sell any patented invention that may in any way be related thereto.

Qualified users may obtain copies of this report from the Defense Documentation Center.

References to named commercial products in this report are not to be considered in any sense as an endorsement of the product by the United States Air Force or the Government.

EXPERIMENTAL VERIFICATION OF A TECHNIQUE FOR TESTING FULL-SCALE INLET/ENGINE SYSTEMS AT ANGLES OF ATTACK UP TO 20 DEG AT TRANSONIC SPEEDS

R. L. Palko
ARO, Inc.

FOREWORD

The work reported herein was conducted by the Arnold Engineering Development Center (AEDC), Air Force Systems Command (AFSC), under Program Element 65802F. The technical monitoring of the effort was performed by Capt. Carlos Tirres, USAF, R & D Division, Directorate of Technology.

The results of research presented were obtained by ARO, Inc. (a subsidiary of Sverdrup & Parcel and Associates, Inc.), contract operator of AEDC, AFSC, Arnold Air Force Station, Tennessee. The investigation was conducted from July 1, 1972, to June 30, 1973, under ARO Project No. PF218. The manuscript was submitted for publication on August 24, 1973.

Acknowledgment is made of the assistance of Mr. J. L. Jacocks of the Propulsion Wind Tunnel Facility, 16T/S Projects Branch, who did the dynamic pressure analysis and flow angularity probe calibration analysis and Mr. W. P. Harmon of the Propulsion Wind Tunnel Facility, Test Operations Branch, who designed the test equipment.

This technical report has been reviewed and is approved.

CARLOS TIRRES
Captain, USAF
Research and Development Division
Directorate of Technology

ROBERT O. DIETZ
Director of Technology

ABSTRACT

A study was conducted to demonstrate experimentally the capability of a new flow-shaping technique to extend the full-scale inlet/engine testing limit of the AEDC 16-Ft Transonic Wind Tunnel. Simulation was accomplished up to 20-deg angle of attack using a pair of modified hollow cylinder, flow-shaping devices and a 1/16-scale inlet model in the AEDC 1-Ft Transonic Wind Tunnel. This is an increase of 8 deg in pitch over the present geometric pitch limit of 12 deg. Inlet ramp and lip pressure data were used to verify the technique supported by Mach numbers measured in front of the inlet, pressures measured at the engine-face station, and inlet dynamic total-pressure data. The Mach number range covered by the study was from 0.6 to 1.1.

CONTENTS

APPENDIXES

I. ILLUSTRATIONS

Figure

NOMENCLATURE

K_θ	Circumferential distortion factor
L_n	Inlet lip pressure orifice number, (n = 1...3)
M_∞	Free-stream Mach number

M_p	Flow angularity probe Mach number
M_s	Simulated Mach number
p/p_{t_∞}	Ratio of surface static pressure to free-stream total pressure
p_{t_E}	Local probe total pressure at engine-face station
$p_{t_E}/p_{t_{E\,MAX}}$	Probe total pressure at engine-face station to highest local probe total pressure at engine-face station
$\overline{p_{t_2}}/p_{t_\infty}$	Average steady-state inlet total-pressure recovery
R_n	Inlet ramp pressure orifice number, (n = 1...5)
ϵ	Upwash angle, deg, positive up
δ	Sidewash angle, deg, positive away from fuselage

SECTION I
INTRODUCTION

Full-scale inlet/engine testing in the AEDC 16-Ft Transonic Wind Tunnel (PWT-16T) has been limited to approximately 12-deg angle of attack because of the physical size of the inlet/engine systems. This limit is illustrated in Fig. 1 (Appendix I) where the schematic depicts a typical present-day inlet/engine system installed in the PWT-16T Tunnel. Since many of these systems are expected to operate efficiently up to angles of attack of 25 deg in the transonic Mach number range, many system problems and limitations may not become evident when testing is limited to 12-deg angle of attack.

The impact of the angle-of-attack limitation is graphically shown in Fig. 2, taken from Ref. 1, which gives the inlet total-pressure recovery ($\overline{p_{t_2}}/p_{t_\infty}$) and engine-face circumferential distortion ($K\theta$) versus angle of attack at Mach numbers of 0.9 and 1.2 from a scale model test of a typical high-performance aircraft configuration. For this particular inlet configuration, extrapolation of the total-pressure recovery from a limit of 10 to 12 deg would indicate that the recovery would not drop below 96 percent at a Mach number of 0.9 and would drop to near 90 percent at an angle of attack of 25 deg for a Mach number of 1.2. However, the sub-scale test data obtained at 25-deg angle of attack showed just the opposite trend with the recovery at Mach 0.9 dropping to approximately 93 percent and with the recovery at Mach 1.2 remaining above 95 percent. The circumferential distortion factor does indicate a rise prior to the angle cutoff limit but does not present a potential problem until after the angle limit is reached. In either case, it is desirable to test the full-scale system to higher angles of attack to verify such sub-scale testing when developing a high-performance aircraft either piloted or unpiloted.

A new wind tunnel large enough to conduct tests at the desired high angles of attack would be rather costly. Therefore, modification to existing facilities might be preferred at a considerably lower cost. To meet this challenge, a research effort was undertaken in 1970 to develop a technique to test full-scale inlet/engine systems at high angles of attack in the existing PWT-16T Wind Tunnel. The first significant results of this effort are reported in Refs. 2, 3, and 4. Conclusions derived from these results indicate that a technique of actually shaping (or deflecting) the airflow in the vicinity of the inlet to simulate the flow field which would occur in free flight at angles of attack up to 20 deg were not only aerodynamically possible but were physically feasible in the PWT-16T. The results were obtained from sub-scale testing in the AEDC 1-Ft Transonic Wind Tunnel (PWT-1T). This new technique will fill a significant portion of the gap between the present maximum test capability limit and the desired test capability as shown in Fig. 3.

Although the research reported in Refs. 2, 3, and 4 showed the technique was possible, it was still necessary to demonstrate that the technique could duplicate the inlet flow in conjunction with an actual inlet model. The research effort for FY'73 was devoted to this end. Only the pitch capability demonstration was attempted. The demonstration of pitch-yaw combinations will be attempted at a later date.

This report presents the results of the verification study.

SECTION II
EXPERIMENTAL VERIFICATION OF SIMULATION TECHNIQUE

The method used to verify the inlet flow simulation capability of the technique was to first obtain experimental data on the inlet/engine simulation model (inlet model) at several angles of attack up to the physical limit obtained in the wind tunnel which, for the model used, was 12-deg pitch. (This configuration is shown in Fig. 4.) These data were duplicated using the inlet model set at 2-deg angle of attack and a flow-shaping device. After the duplication was accomplished, a combination of geometric pitch angles and flow-shaping positions was used to extend the pitch angle limit up to 20 deg. Since the previous studies (Refs. 3 and 4) had shown the dual, modified hollow cylinder, shaping device (modified cylinders) to have the best overall flow-shaping characteristics, this device was used for the experimental verification of the technique. (This experimental configuration is shown in the wind tunnel in Fig. 5.)

Pressure measurements on the inlet ramp and lip, supported by flow angularity probe data in front of the inlet, were used as the basis for proving that duplication of the inlet data was accomplished. In addition to the inlet pressure measurements, engine-face station total-pressure measurements were made as a secondary indication of flow duplication, and the fluctuating total pressure was measured at the inlet throat and in the test section forward of the inlet to verify that the flow-shaping device did not produce any acoustic or velocity disturbances above those already present in the tunnel flow.

SECTION III
APPARATUS

3.1 WIND TUNNEL (AEDC PWT-1T)

The AEDC PWT-1T is a continuous flow, nonreturn, transonic wind tunnel equipped with a two-dimensional, flexible nozzle and a plenum evacuation system. The test section Mach number range can normally be varied from 0.2 to 1.50. Total-pressure control is not available, and the tunnel is operated at a stilling chamber total pressure of about 2850 psfa with a ±5-percent variation depending on tunnel resistance and ambient conditions. The stagnation temperature can be varied from 80 to 120°F above ambient temperature when necessary to prevent moisture condensations in the test region.

The general arrangement of the tunnel and its associated equipment is shown in Fig. 6, and a schematic of the nozzle, test section, and wall geometry is shown in Fig. 7.

3.2 FLOW-SHAPING DEVICE (MODIFIED CYLINDERS)

The modified cylinders are basically two hollow, half-circular cylinders which have been split and widened in the middle by the width of one radius. The dimensions and

shape of an individual cylinder are given in Fig. 8. Each cylinder could be remotely pitched through a continuous angle range from 0 to 35 deg. The distance from the tunnel wall and the spacing between the cylinders could be varied manually, and the yaw angle of Cylinder No. 1 in Fig. 9 could be set at 0, 5, or 10 deg manually. The position of the cylinders is shown schematically in Fig. 9 and in the photograph in Fig. 5. A more complete description of the modified cylinders may be found in Ref. 4.

3.3 INLET MODEL

The inlet model used was a 1/16-scale, two-dimensional, supersonic inlet which was available from a previous wind tunnel blockage study. The model could be manually positioned in the tunnel to place the center of the inlet on the tunnel centerline or one inch below the centerline. The model could also be manually pitched from 0 to 12 deg in 1-deg increments. Flow through the inlet could be varied by a control valve in the scavenging scoop line to simulate the proper airflow for different engine power settings.

Three interchangeable forebody configurations were available. The basic shape of these forebodies is shown in Fig. 10. The short forebody configuration was used during the full-scale inlet/engine test. The N-2 forebody has the same shape as the short forebody but is sliced along the line shown in the bottom view to reduce tunnel blockage. The N-1 forebody is a forebody with a very sharp edge along the front and bottom to restrict the flow from turning toward the fuselage side of the inlet.

Pressure orifices were located along the inlet ramp and lip in the positions shown in Fig. 10. The pressure measurements taken from these orifices were used as the primary indication of flow simulation. A small, nine-probe rake was installed at the engine-face station location in the inlet model for measuring the total-pressure distribution. A photograph of this rake is shown in Fig. 11.

The fluctuating total-pressure measurements were made with a 0.125-in.-diam semiconductor strain-gage transducer mounted in a 1/4-in.-diam tube. One probe was installed in the inlet throat on a support as shown in Fig. 12. A second probe was installed 1 in. from the tunnel wall and 5 in. from the tunnel throat to sense the free-stream total pressure.

3.4 FLOW ANGULARITY PROBE

A flow angularity probe was used to survey the flow field between the modified cylinders and to measure the local flow conditions in front of the inlet. Details of the probe are shown in Fig. 13. This probe was 1/4 in. in diameter and was calibrated in the AEDC PWT-1T over a Mach number range from 0.5 to 1.2. A probe drive system was used to remotely position the probe from the tunnel wall to the tunnel centerline at a station where the probe tip was near the leading edge of the inlet ramp. The installation position of the probe is shown schematically in Fig. 9 and in the photographs in Figs. 4 and 5.

3.5 INSTRUMENTATION

PWT-1T is equipped with a permanently installed, automatic, data recording system. A PDP 11-20 computer provides on-line data reduction. Reduced data are displayed on a line printer, and a high-speed paper tape punch records and stores raw data for the purpose of later off-line analysis.

The pressure data are measured with differential pressure transducers referenced to the tunnel plenum pressure. Analog signals from the transducers are fed through a switch gain amplifier and then through an Analog-to-Digital (A to D) converter to be digitized. The A to D converter uses 12 bits plus sign or 4096 counts full scale. The digital signal from the converter is processed by the PDP 11-20 computer.

The fluctuating total-pressure measurements were made utilizing two 0.125-in.-diam semiconductor strain-gage transducers referenced to the wind tunnel total pressure (p_{t_∞}). The transducer output signals were recorded on magnetic tape using frequency modulation of 500-kHz carriers with a resultant bandwidth of 10 kHz. Although directly coupled, the d-c signal levels were suppressed to avoid saturation of the tape recorder electronics. Overall signal-to-noise ratios were approximately 30 db as determined from wind-on/wind-off measurements with predominant noise attributable to 60-/120-Hz ripple in the transducer power supply. Recording levels were monitored on-line utilizing oscilloscopes and true root-mean-square instrumentation. Subsequent data reduction was accomplished on a special-purpose digital spectral analyzer with an ensemble averaging in the frequency domain yielding 40-degree-of-freedom spectral density estimates.

SECTION IV
RESULTS AND DISCUSSION

To verify the new flow-shaping technique for testing full-scale inlet/engine systems at high angles of attack, it was first necessary to obtain data on a basic inlet model configuration at known geometric pitch angles and wind tunnel free-stream Mach numbers. The basic configuration chosen was the inlet model with the N-2 forebody as described previously (see Fig. 10).

Inlet ramp and lip pressure data taken with the basic configuration at geometric pitch angles of 0, 4, 8, and 12 deg and free-stream Mach numbers of 0.6, 0.7, 0.8, 0.9, 1.0, and 1.1 are shown in Fig. 14a through f, respectively. The configuration code number used in the figure had a significance during the experimental study but not in this report and is given only to allow correlation between the figures and the configuration settings given in Table I (Appendix II). The data are presented as a ratio of the inlet static to the free-stream total pressure. The general trend of the data show that an increase in free-stream Mach number resulted in a decrease in the inlet ramp and lip static pressure, and an increase in pitch angle resulted in an increase in the inlet ramp and lip static pressure.

Since an increase in ramp and lip pressure could indicate either a lower free-stream Mach number or a higher pitch angle, it is necessary to know that either the local Mach number or pitch angle is simulated correctly if simulation of the other is to be obtained. Previous flow angularity survey data showed that the process of deflecting the flow upward for angle-of-attack simulation also changed the local Mach number. Therefore, in an attempt to assure that one of the necessary variables was simulated, flow angularity and local Mach number data were obtained approximately 4 in. forward and in the vertical plane of the inlet lip using the flow angularity probe. Two sets of data points were actually taken at each condition, one with the probe located at the point indicated above for the Mach number and flow angularity data and one with the probe withdrawn to the wall for the inlet ramp and lip pressure data. This was necessary because probe interference was present in the ramp and lip static pressure when the probe was inserted in front of the inlet lip.

The flow angularity probe data for the basic inlet configuration are shown in Fig. 15. These data show that the local Mach number decreased in front of the inlet and that the decrease was greater as the pitch angle increased. The data also show that the inlet tended to deflect the flow downward approximately 3 deg, relative to the inlet axis, so that a 0-deg pitch angle gave a 3-deg downwash angle, and a 12-deg pitch angle gave a 9-deg upwash angle. The sidewash angle decreased as the inlet was pitched to angle of attack.

To reproduce the data obtained with the basic inlet model configuration at angles of attack of 8 and 12 deg using the modified cylinders for flow shaping, the N-1 forebody was used with the inlet model. It was originally intended that no forebody would be used during the simulation study; however, the flow angularity probe data taken during the blockage phase in Ref. 4, where the probe was attached to the inlet model to measure the effect of the presence of the inlet, showed that an inflow toward the fuselage side of the inlet was present with the forebody removed. This is an impossible condition since the fuselage would block the flow in this direction. Therefore, a forebody designated N-1 (Fig. 10) was installed on the inlet model during the simulation study. This forebody is described in Section 3.3 and was used in place of the N-2 forebody because it gave greater maneuvering area in the tunnel test section for the modified cylinders.

Prior to attempting to simulate the basic model configuration data, plots were made of the tunnel free-stream Mach number and upwash angle versus probe Mach number using data taken with the modified cylinders alone during the study reported in Ref. 4. These data (Fig. 16) were taken at the horizontal centerline of the tunnel offset from the vertical centerline to match the center of the inlet. It was hoped that these data could be used to pick the correct wind tunnel free-stream Mach number and cylinder pitch angle settings for any desired Mach number and pitch angle to be simulated. For example, from Fig. 16, to produce a simulated pitch angle of 8 deg and a Mach number of 0.8 would require a free-stream Mach number of 0.69 with the cylinders each set at 27-deg pitch. This was obtained by first determining the cylinder pitch angle requirement from the probe Mach number versus upwash angle curve at a Mach number of 0.8 and an upwash of 8 deg

and then at this cylinder pitch setting (27 deg) and probe Mach number 0.8 determine the free-stream Mach number from the probe Mach number versus free-stream Mach number curve. However, Fig. 15 shows that a local Mach number of approximately 0.71 and an upwash angle of approximately 5.4 deg is required for correct simulation which indicated the need for a free-stream Mach number of 0.68 with the cylinders set at something less than 10-deg pitch using the same method of determination. Neither of these settings produced the correct simulation. It was found that in order to produce the correct sidewash component it was necessary to yaw Cylinder No. 1 (nose away from the tunnel center), see Fig. 9. Since only limited data were available with the Cylinder No. 1 yawed, this method of predetermining the tunnel free-stream Mach number and cylinder pitch angle settings for different simulation conditions was of little value. Therefore, the settings were determined by trial and error and experience gained during the study.

Using the lip and ramp pressure distribution and local Mach number in front of the inlet for the basic configuration at pitch angles of 8 and 12 deg, the wind tunnel free-stream Mach number and the modified cylinder pitch angles were varied until a match of the inlet ramp and lip pressure, and local Mach number was obtained between the basic configuration data and the simulated data. Assuming that the initial settings were close, which was true in most cases, if the ramp and lip pressure were both off in the same direction, then the free-stream Mach number needed to be varied either up or down. That is if the ramp and lip pressure were both high, it was necessary to increase the free-stream Mach number; if they were both low, it was necessary to decrease the Mach number in order to obtain simulation. On the other hand, if either the ramp or lip pressure was high and the other low, then it was necessary to change the cylinder pitch angle to obtain simulation. Usually some adjustment was required in both cylinder pitch angle and free-stream Mach number to get the desired simulation.

Using the on-line data reduction capability of the PWT-1T, it was possible to continuously compare the simulated data with the basic data until the desired match was observed. To position the inlet between the cylinder for best results, it was necessary to pitch the inlet model to 2-deg angle of attack. The final settings of free-stream Mach number and cylinder pitch angle needed to simulate a given flight pitch angle and Mach number are given in Table 1. The comparisons between the basic configuration and the flow-shaping configuration ramp and lip pressure data for pitch angles of 8 and 12 deg are shown in Figs. 17 and 18. In trying to adjust the wind tunnel free-stream Mach number and cylinder pitch angle to get the desired simulation, emphasis was put on matching the pressure measured at the last orifice on the inlet ramp (R_5) and the first orifice on the lip (L_1) since these were nearly on opposite sides of the inlet throat. It was assumed if the pressure was matched on both sides of the inlet throat for both configurations, it was very likely that the flow into the inlet was the same. The data show that excellent agreement was obtained at both pitch angles for Mach numbers 0.6, 0.7, and 0.8 with slight deviation occurring at Mach number 0.9, and the deviation increased at Mach numbers 1.0 and 1.1. However, the agreement at Mach number 1.1, which showed the greatest deviation, can still be termed good. The solid symbols in Figs. 18e and f indicate that different cylinder positions were required to obtain simulation at Mach numbers of 1.0 and 1.1.

As discussed earlier in this section, the effect of changes in Mach number and pitch angle are such that it is necessary to know that one of these parameters is correct if the other is to be assumed correct when the inlet ramp and lip pressure are matched. Since the flow surveys between the modified cylinders showed that the variations in upwash angle were larger than the variations in local Mach number, the Mach number and inlet ramp and lip pressure data were used as a basis of proof that pitch angle was simulated. For each group of data taken to obtain inlet ramp and lip pressure, a corresponding group of data was taken with the flow angularity probe in front of the inlet to obtain the local Mach number. The flow angularity probe data for the 8- and 12-deg simulation are shown in Figs. 19 and 20, respectively. The data in these figures show that a difference in local Mach number does exist between the data taken with the basic configuration and the flow-shaping configuration. However, the inlet data taken during the cylinders-only study (Ref. 4), showed that the local Mach number increased as the probe was moved upward between the cylinders from the bottom to the top (Fig. 21). It should be noted from the sketch in Fig. 22 with the cylinders installed that the probe tip is approximately 1-in. below the centerline of the cylinders when they are pitched either 20 or 30 deg, whereas the centerline of the inlet is approximately 1 to 1.5 in. above the centerline of the cylinders for the same pitch angles. When the difference in Mach number from the probe location to the center of the cylinders (this appears to be a mean forebody shielding point as shown in Fig. 9) is taken from Fig. 21 and applied to the data in Figs. 19 and 20, good agreement is shown between the two sets of data (see solid symbols on Figs. 19 and 20). Although emphasis was placed on matching the local Mach number, a similar correction can be applied to the upwash and sidewash data which gives the corrected values shown on Figs. 19 and 20 with the solid symbols.

To obtain simulation at 16-deg angle of attack, the inlet model was pitched to 10 deg, and the free-stream Mach number and cylinder pitch settings for 8-deg simulation were used (see Table I). Since 2-deg pitch of the inlet model was required for the 8-deg simulation, this gave an additional 8 deg of pitch. In order to position the inlet near the same cylinder location, as was present in the 8-deg simulation, the inlet model was shifted 1 in. nearer the threoretical bottom of the tunnel. The PWT-1T is actually turned on its side with respect to the PWT-16T. Since the basic data could not be obtained at a pitch angle of 16 deg due to the 12-deg physical limit of the tunnel, comparison is made with an extrapolated curve (see Fig. 23) taken from the basic configuration data in Fig. 14. The simulation data for 16-deg pitch are shown in Fig. 24. The ramp pressures show excellent agreement over the Mach number range; however, there is a deviation in the lip pressures at Mach numbers of 1.0 and 1.1.

To obtain simulation at 20-deg angle of attack, the inlet model was pitched to 10 deg, and the free-stream Mach number and cylinder pitch settings for 12-deg simulation were used (Table I). With the 2-deg pitch required during the 12-deg simulation, this again gives an additional 8 deg of pitch. The inlet model was positioned at the same tunnel location as used in the 16-deg simulation. The simulation data for 20-deg pitch are shown in Fig. 25. Here again, the comparison is made with an extrapolated curve obtained from Fig. 14. Again, the ramp pressures showed excellent agreement over the Mach number range with deviation in the lip pressures occurring at Mach numbers of 1.0 and 1.1.

As a secondary indication of flow simulation, data were taken with a nine-probe pressure rake located at the engine-face station in the inlet duct (Fig. 11). Since the inlet model was a 1/16-scale, fixed ramp angle model of an inlet designed for a variable ramp angle, it was not expected that inlet recovery would correctly duplicate the actual full-scale inlet configuration, but rather would indicate if any major deviations were present between data taken on the basic inlet configuration and data taken during flow simulation. The average total pressure measured with only eight of the nine probes on the rake versus pitch angle for the basic model is shown in Fig. 26 for the various test Mach numbers. These data show that the small scale and fixed ramp angle had poor pressure recovery and produced a trend with pitch angle reversed from that of the much larger scale (1/4-scale) variable ramp inlet of Fig. 2. However, the data taken with the basic inlet and the simulated data have generally the same trends as shown in Fig. 27 with a maximum deviation of two percent in total-pressure recovery. Total-pressure profiles at the compressor-face station are shown in Fig. 28. These data are presented as lines of constant ratios of the local probe total pressure at the engine-face station to the highest local probe total pressure at the engine-face station ($p_{t_E}/p_{t_{E\ MAX}}$). It can be observed that no great difference exists in the flow patterns between the basic configuration data and the simulated data. The variations in the engine-face pressure maps with simulated pitch angle for a Mach number of 0.8 are shown in Fig. 29. Only slight variations are observed with the major variations being in the low-pressure regions.

The fluctuations in total pressure were obtained on eight test configurations to document the effects of flow-shaping devices on inlet turbulence levels and frequency spectra. No significant differences were noted in the dynamic data with any of the variations so that the results presented are limited to the two basic configurations: inlet model pitched to 8 deg with the short forebody (Fig. 10) and simulation with the inlet model set at 0-deg pitch and the modified cylinders pitched 30 deg.

Spectral characteristics of the test section total pressure are presented in Fig. 30 with bandwidths of 500 Hz and 5 kHz. As reported in Ref. 5, the PWT-1T compressor is of the centrifugal type with 18 helical vanes on each side of the impeller and a rotation rate of 3456 rpm which results in a fundamental blade-passage frequency of 1036 Hz. This frequency and its harmonics are strongly evident in all dynamic data acquired. Cross-spectral analysis (not presented here) between the two dynamic pressure probes conclusively show the blade passage disturbance to be airborne rather than transmitted by tunnel structure, although it is not clear whether the disturbance is acoustic or transported with stream velocity. Another significant tunnel disturbance is at the low-frequency (20 Hz) end of the spectrum and is associated with the fundamental organ-pipe resonance of the tunnel ducting. The generation mechanism is simply acoustic coupling between the test section and the downstream tunnel throttle valve located 13.5 ft aft of the test section. The data of Ref. 5 indicate this disturbance is significant only at supersonic Mach numbers, whereas the current results show little variation with Mach number changes. It is suspected that the discrepancy is attributable to the model installation providing a local disturbance in the test section which is then amplified by the acoustic

coupling for the current study, whereas that of Ref. 5 was for an empty tunnel. This hypothesis is supported by the observation that increased tunnel blockage tends to increase the magnitude of low-frequency pressure fluctuations.

Spectral data obtained with the inlet probe are presented in Fig. 31 for the inlet model pitched to 8 deg and in Fig. 32 for the inlet model set at 0 deg with modified cylinders pitched to 30 deg. Little difference is apparent between the free-stream total and the inlet total, and no significant differences exist among the data for the two configurations. The root-mean-square pressure level is nominally 0.35 percent of the absolute pressure (5-kHz bandwidth) at $M_\infty = 0.6$ and increases uniformly to 0.40 percent at $M_\infty = 1.1$ for both configurations. Installation of the cylinders did cause a slight increase in the flow-frequency energy level through interaction with the basic tunnel characteristics, and there is an unexplained attenuation in both the inlet and the free-stream probe data of the compressor blade-passage frequency harmonic at 4 kHz with the cylinders installed.

SECTION V
CONCLUSIONS

Experimental verification of the flow-shaping technique for extending the full-scale inlet/engine testing capability of the PWT-16T up to pitch angles of 20 deg was accomplished. The duplication of the inlet ramp and lip pressure was excellent at Mach numbers of 0.6, 0.7, and 0.8 with only slight deviation occurring at Mach numbers of 0.9, 1.0, and 1.1. Study of the total pressure at the engine-face station location and the total-pressure fluctuations in the inlet throat indicate no adverse effects of using the modified cylinders to simulate high angles of attack.

The interaction between the inlet model and modified cylinder flow-shaping device is such that model testing of each inlet engine configuration will probably be necessary when using this technique for full-scale inlet/engine testing. However, the modified cylinder shape will probably give sufficiently good simulation for most inlet/engine testing for side-mounted inlet configurations.

In addition to controlling the pitch, yaw, and vertical position of the flow-shaping devices, the capability to position the devices laterally in the tunnel is also needed. Vertical positioning of the engine could be used rather than vertical positioning of the modified cylinders.

REFERENCES

1. Lauer, R. F., Jr. "Inlet Performance Characteristics of Generalized 1/4-Scale Tactical Aircraft Models at Transonic and Supersonic Mach Numbers." AEDC-TR-71-87 (AD515022L), May 1971.

2. Palko, R. L. "Full-Scale Inlet/Engine Testing at High Maneuvering Angles at Transonic Velocities." AIAA Paper No. 72-1026, Presented at the AIAA Seventh Aerodynamic Testing Conference, Palo Alto, California, September 13-15, 1972.

3. Palko, R. L. "A Method of Testing Full-Scale Inlet/Engine Systems at High Angles of Attack and Yaw at Transonic Velocities." AIAA Paper No. 72-1097, Presented at the AIAA/SAE Eighth Joint Propulsion Specialist Conference, New Orleans, Louisiana, November 29-December 1, 1972.

4. Palko, R. L. "A Method to Increase the Full-Scale Inlet/Engine System Testing Capability of the AEDC 16-Ft Transonic Wind Tunnel." AEDC-TR-73-9 (AD762912), June 1973.

5. Robertson, J. E. "Measurement of the Pressure Fluctuations in the Test Section of the One-Foot Transonic Tunnel in the Frequency Range From 5 to 1250 CPS." AEDC-TDR-62-109 (AD275400), May 1962.

APPENDIXES

I. ILLUSTRATIONS

II. TABLE

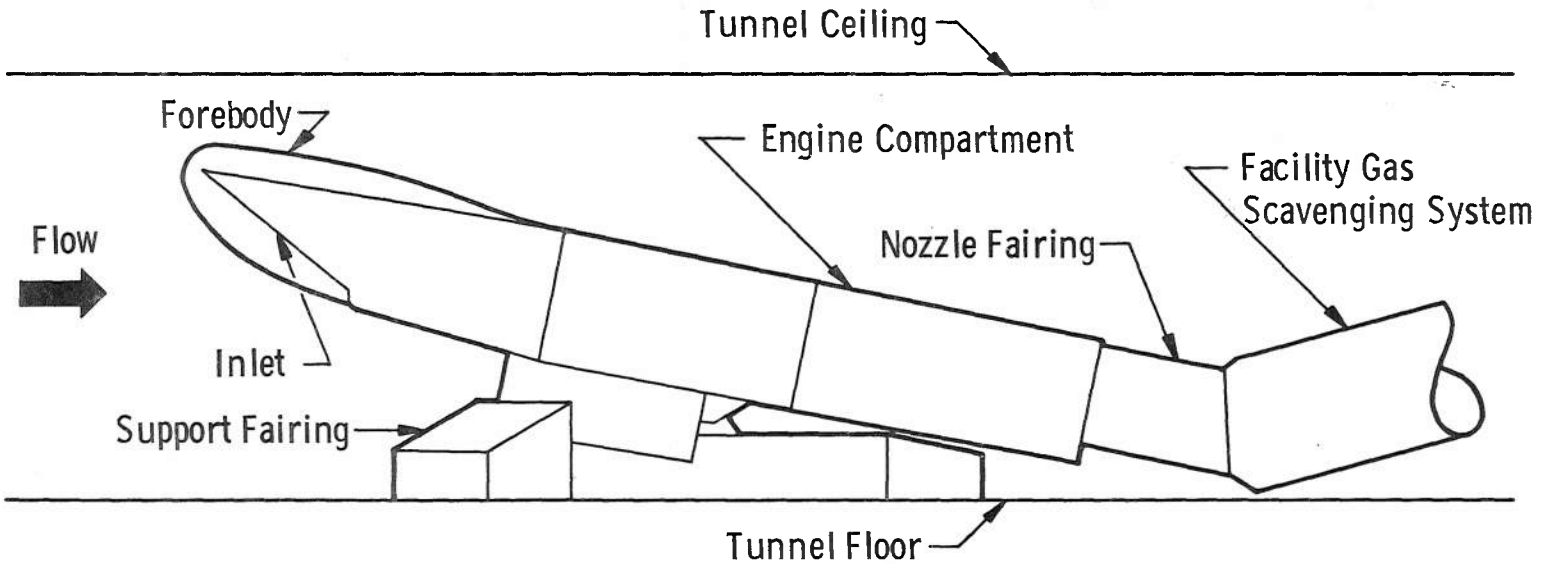

Fig. 1 Typical Full-Scale Inlet/Engine System Installation in the AEDC 16-Ft Transonic Wind Tunnel

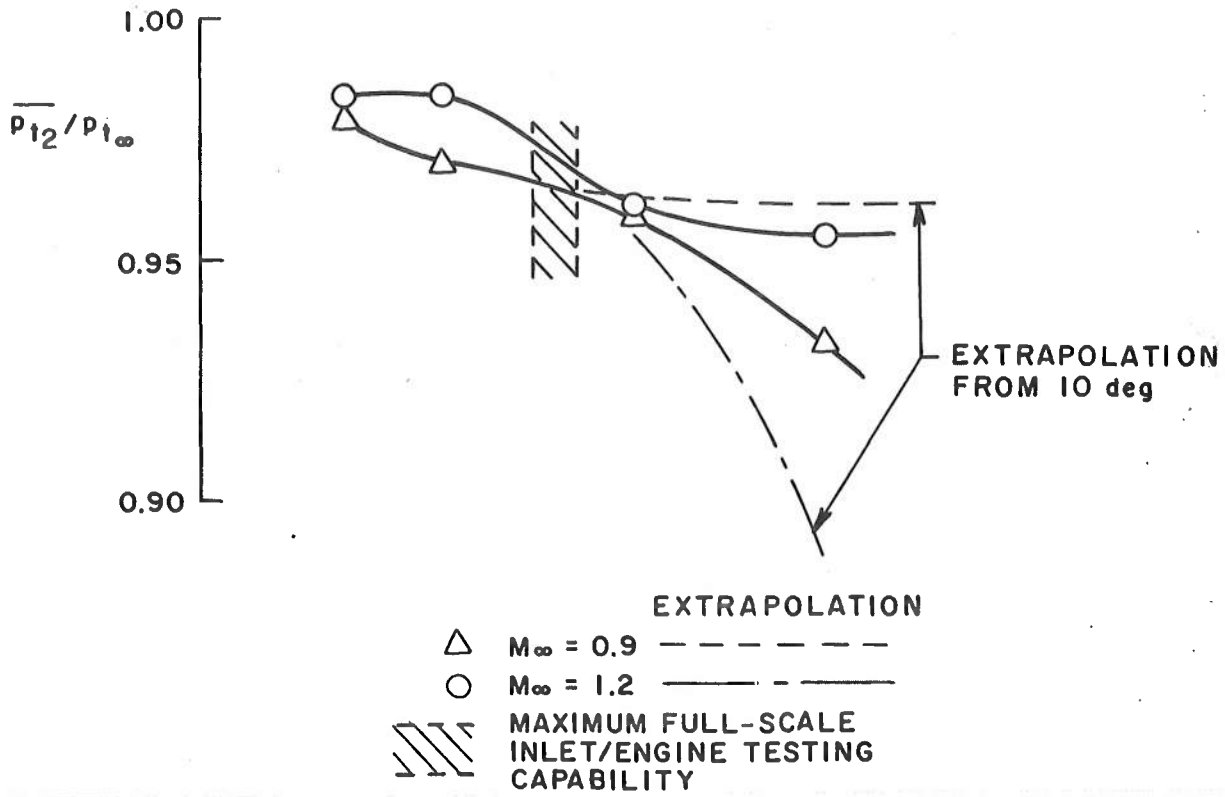

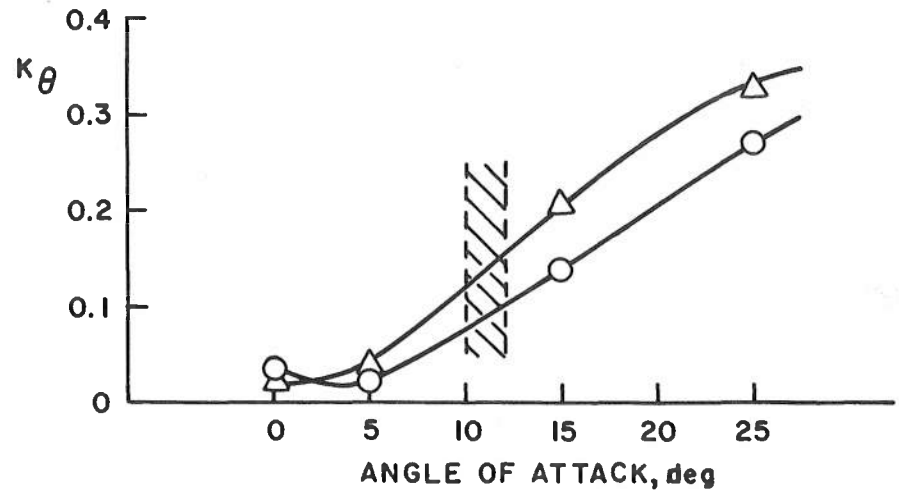

Fig. 2 Inlet Performance for a 1/4-Scale Inlet Model

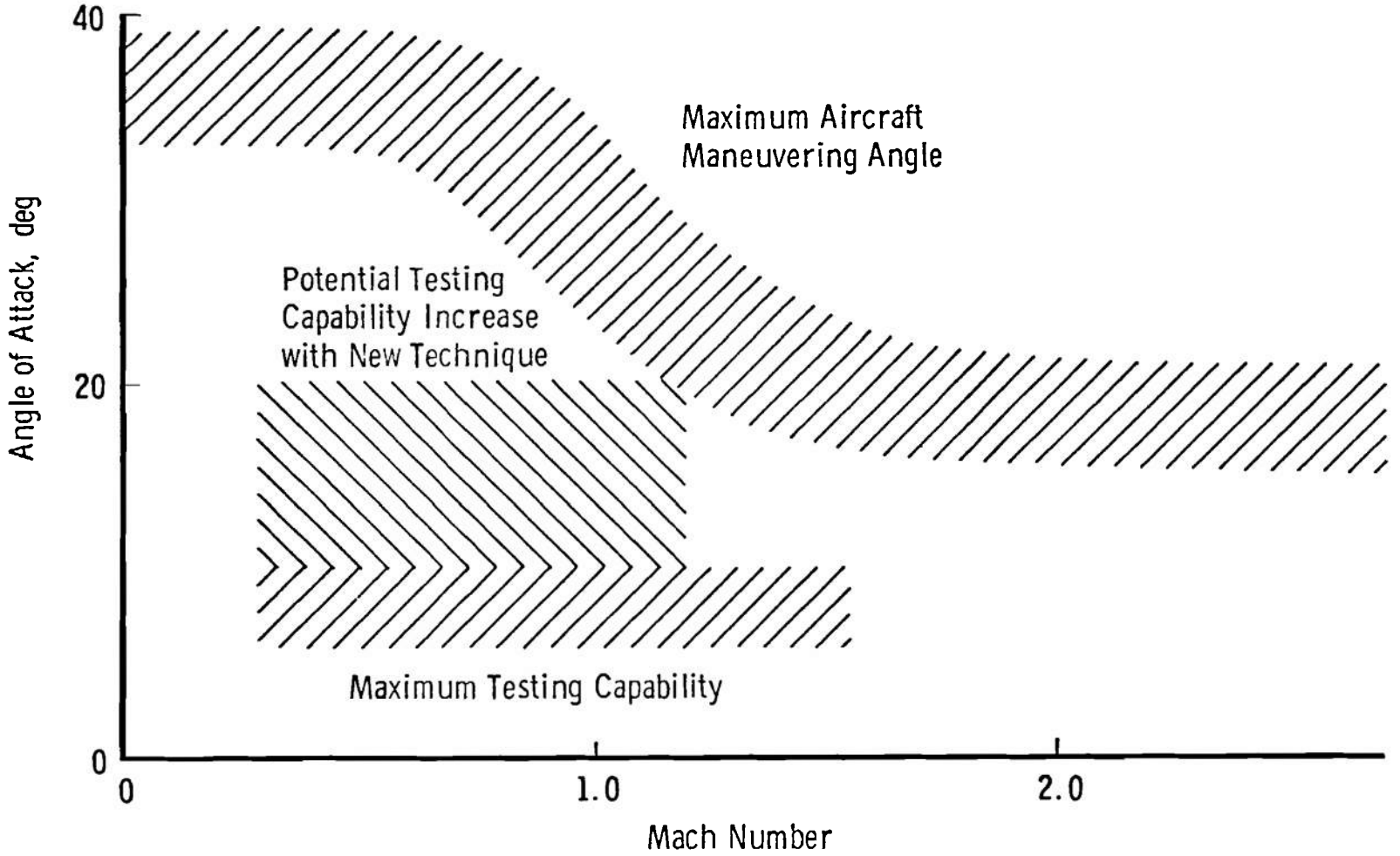

Fig. 3 Comparison of a Typical Highly Maneuverable Aircraft Performance with Present and Potential Wind Tunnel Test Capability

AEDC-TR-73-169

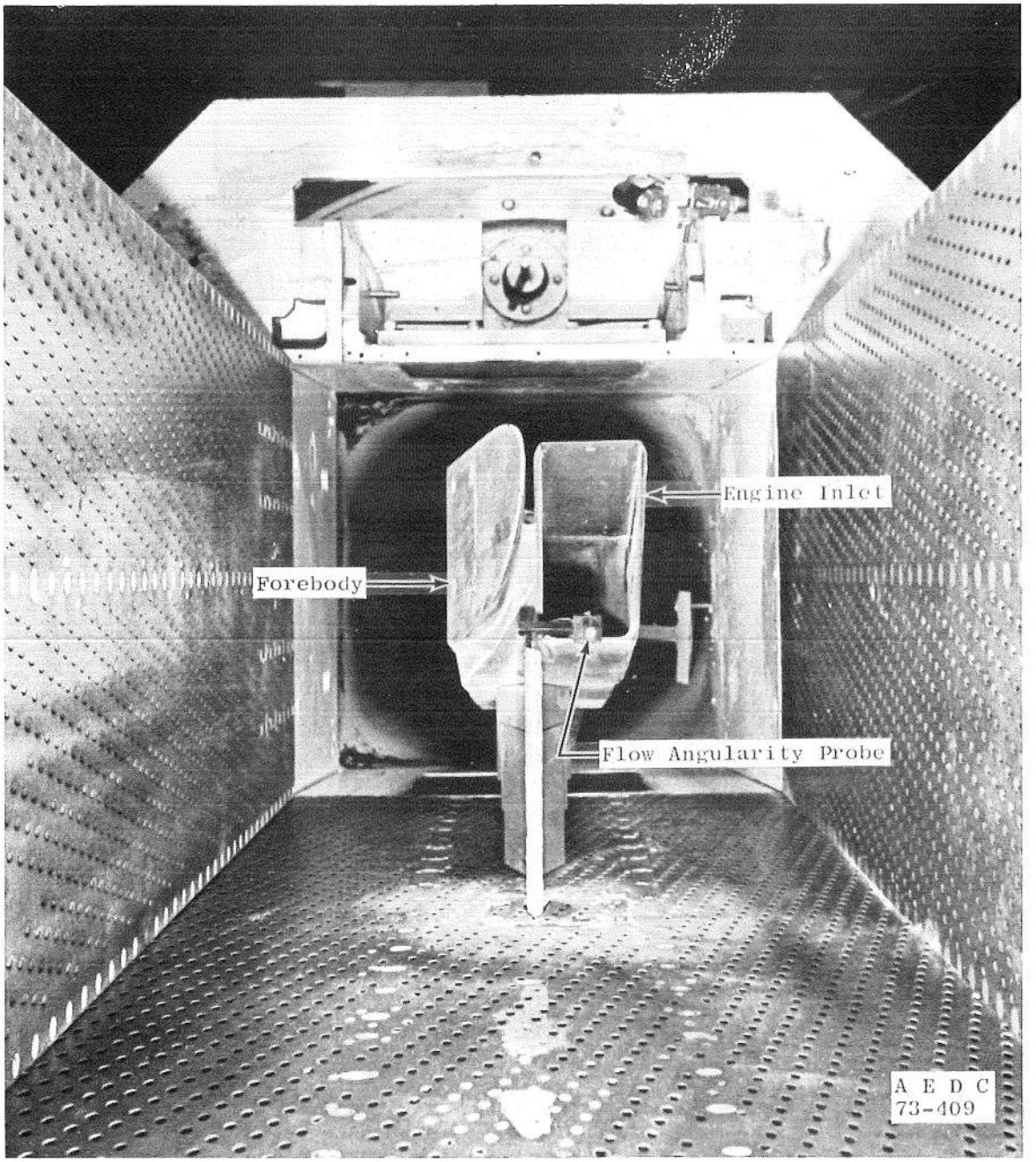

Fig. 4 Installation of Inlet Model with Forebody in the AEDC PWT-1T

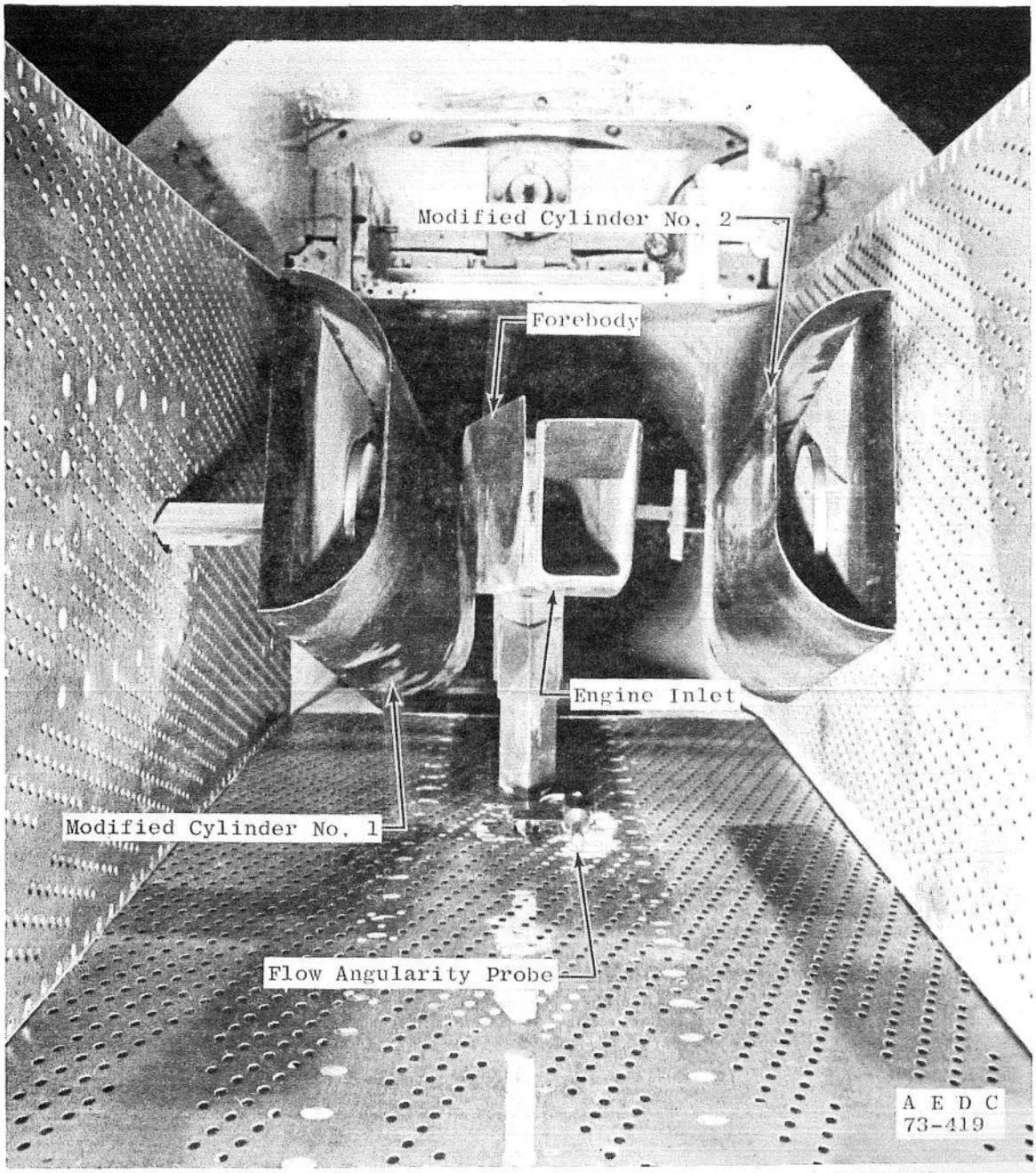

a. Front View

Fig. 5 Installation of Inlet Model with Forebody and Modified Cylinders in the AEDC-PWT-1T

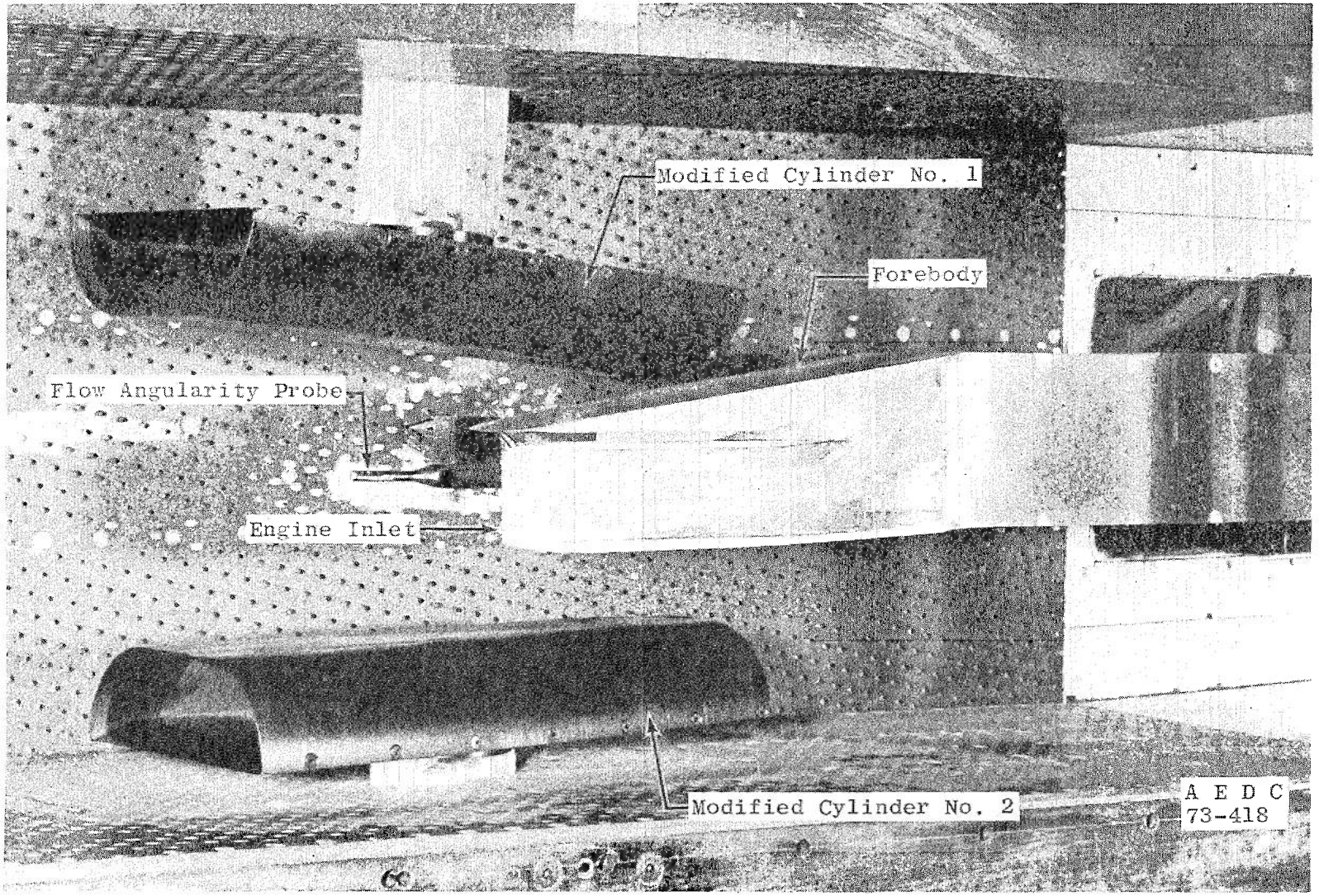

b. View from Top of Inlet Model

Fig. 5 Concluded

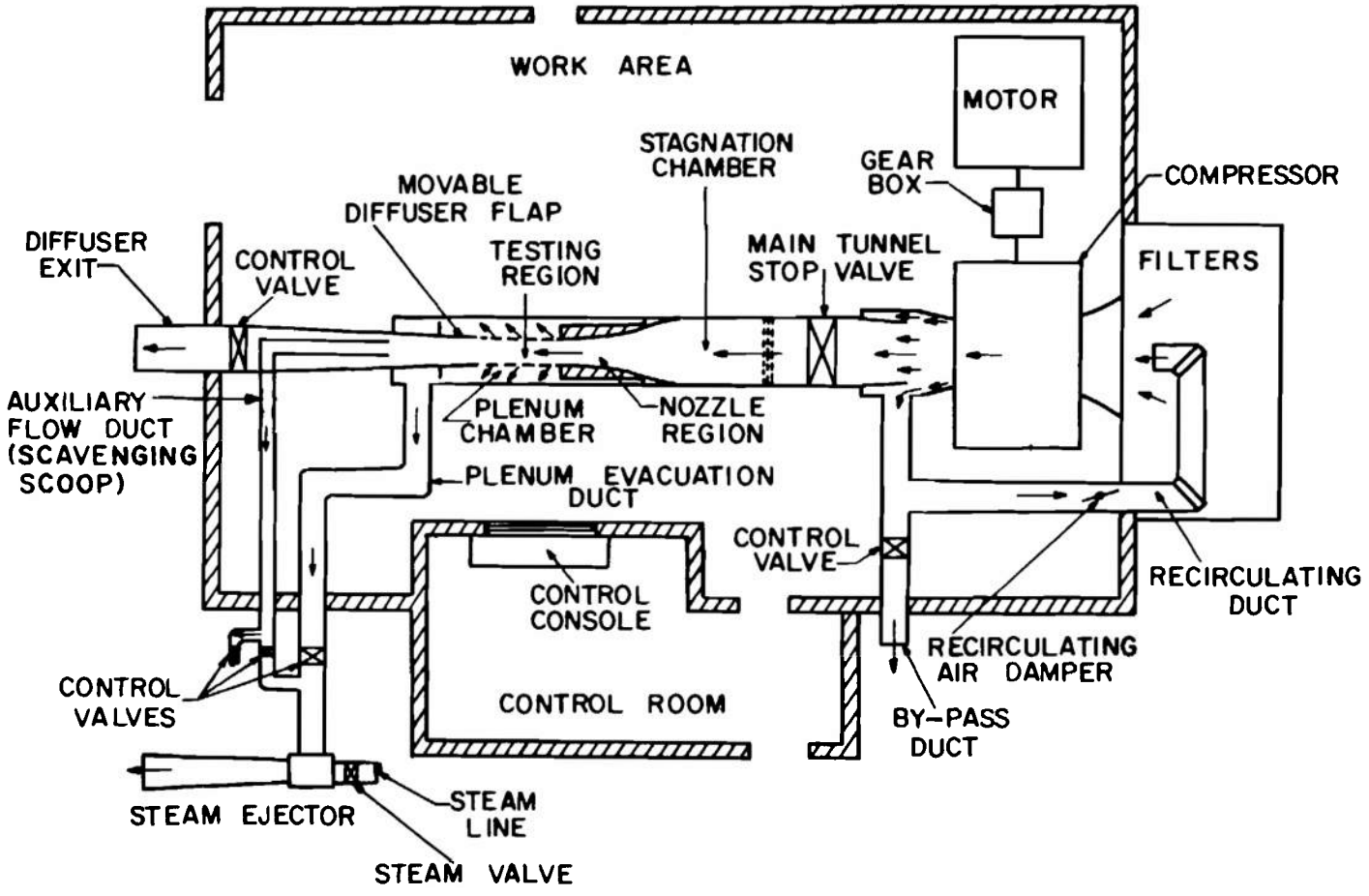

Fig. 6 General Arrangement of the AEDC PWT-1T and Supporting Equipment

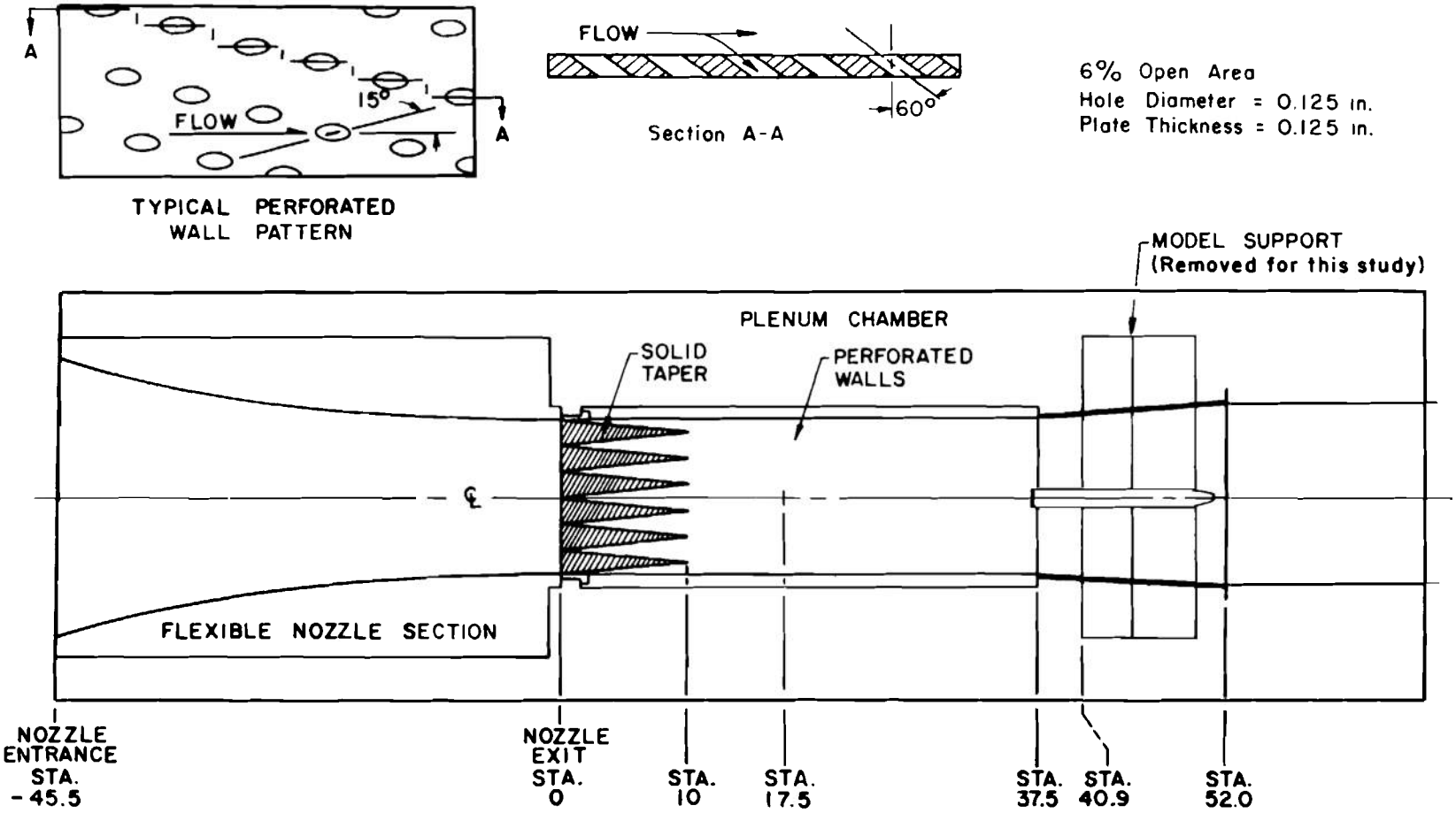

Fig. 7 Schematic of the AEDC PWT-1T Test Leg

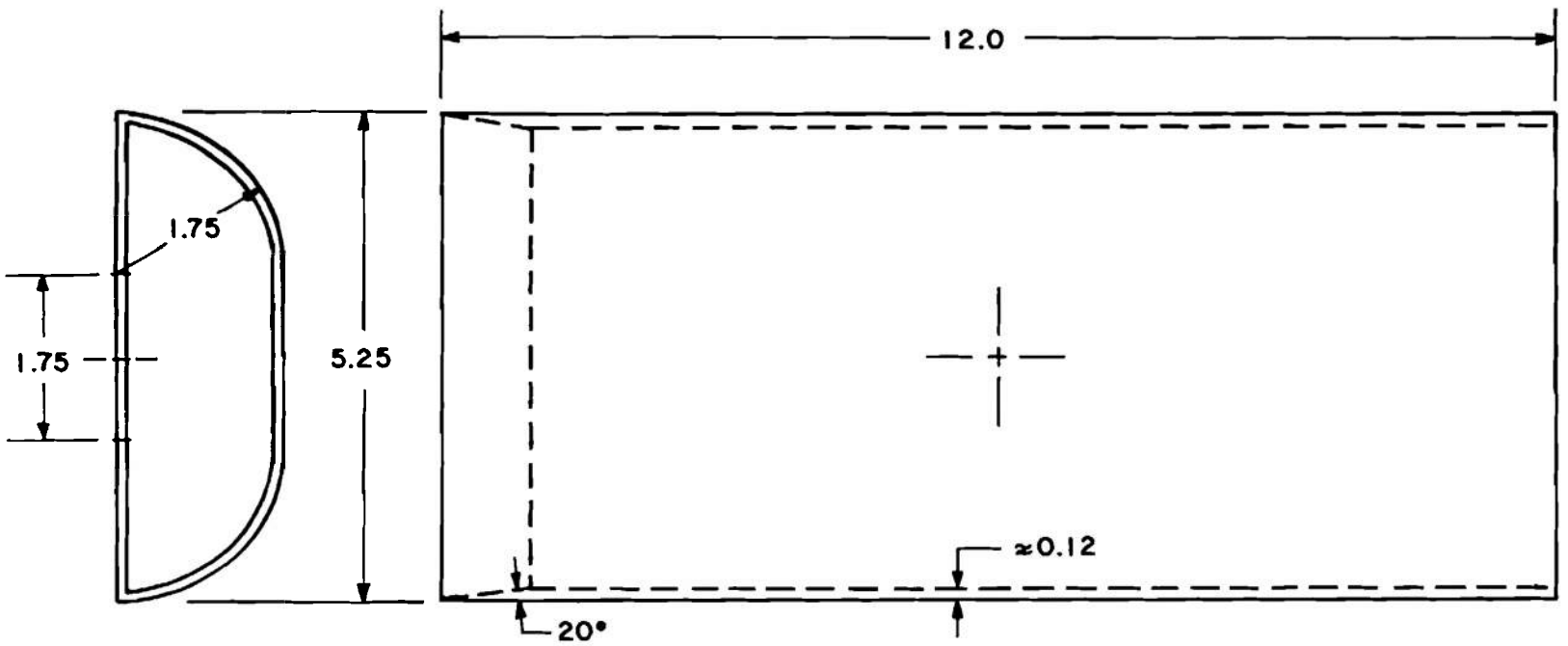

Fig. 8 Schematic of the Modified Cylinder Flow-Shaping Device

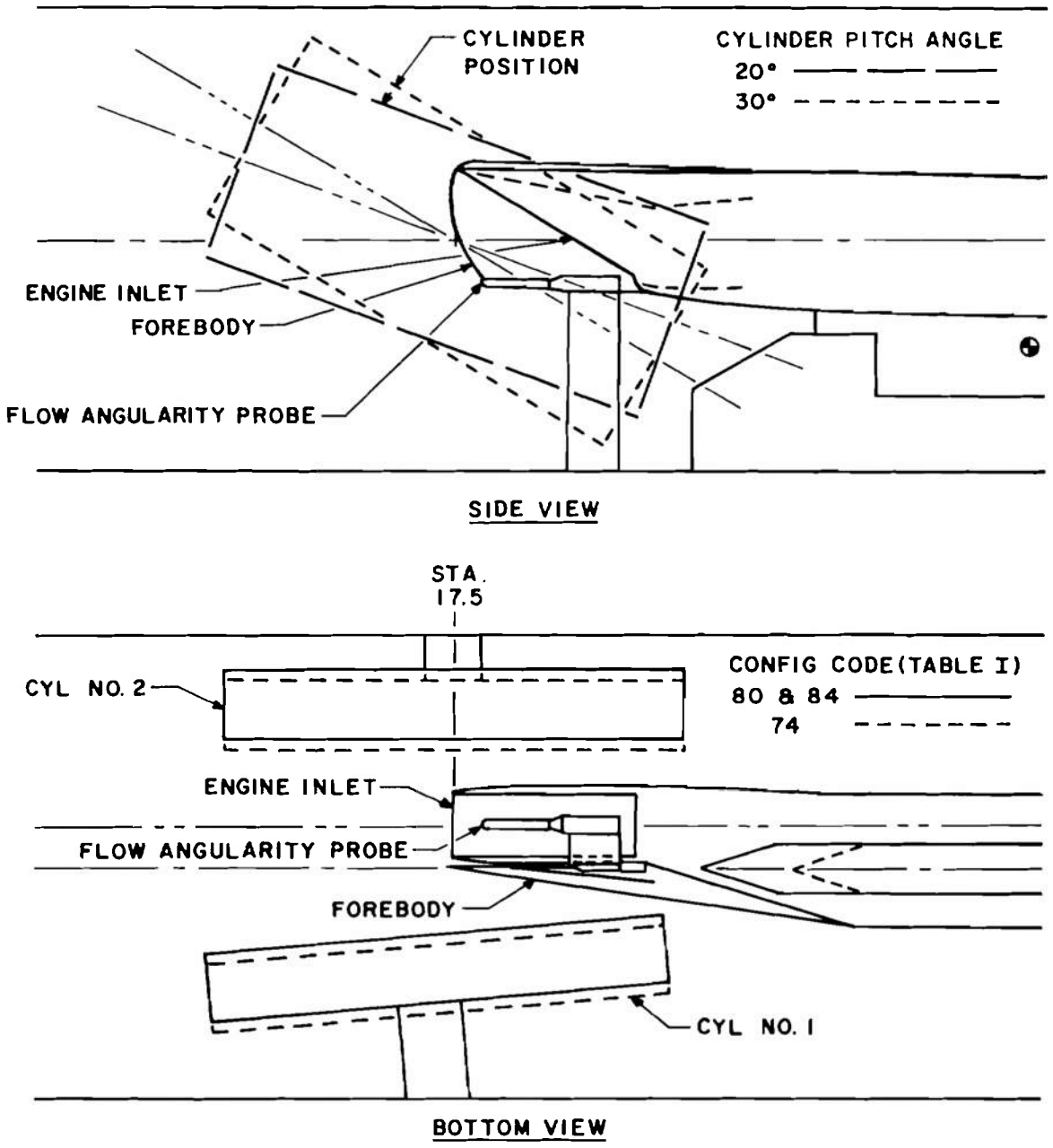

Fig. 9 Schematic of the Model Installation in the AEDC PWT-1T

POSITION FROM TIP OF INLET RAMP, in.
R_1 - 0.45
R_3 - 2.32
R_4 - 3.26
R_5 - 4.20
L_1 - 5.14
L_2 - 5.45
L_3 - 6.07

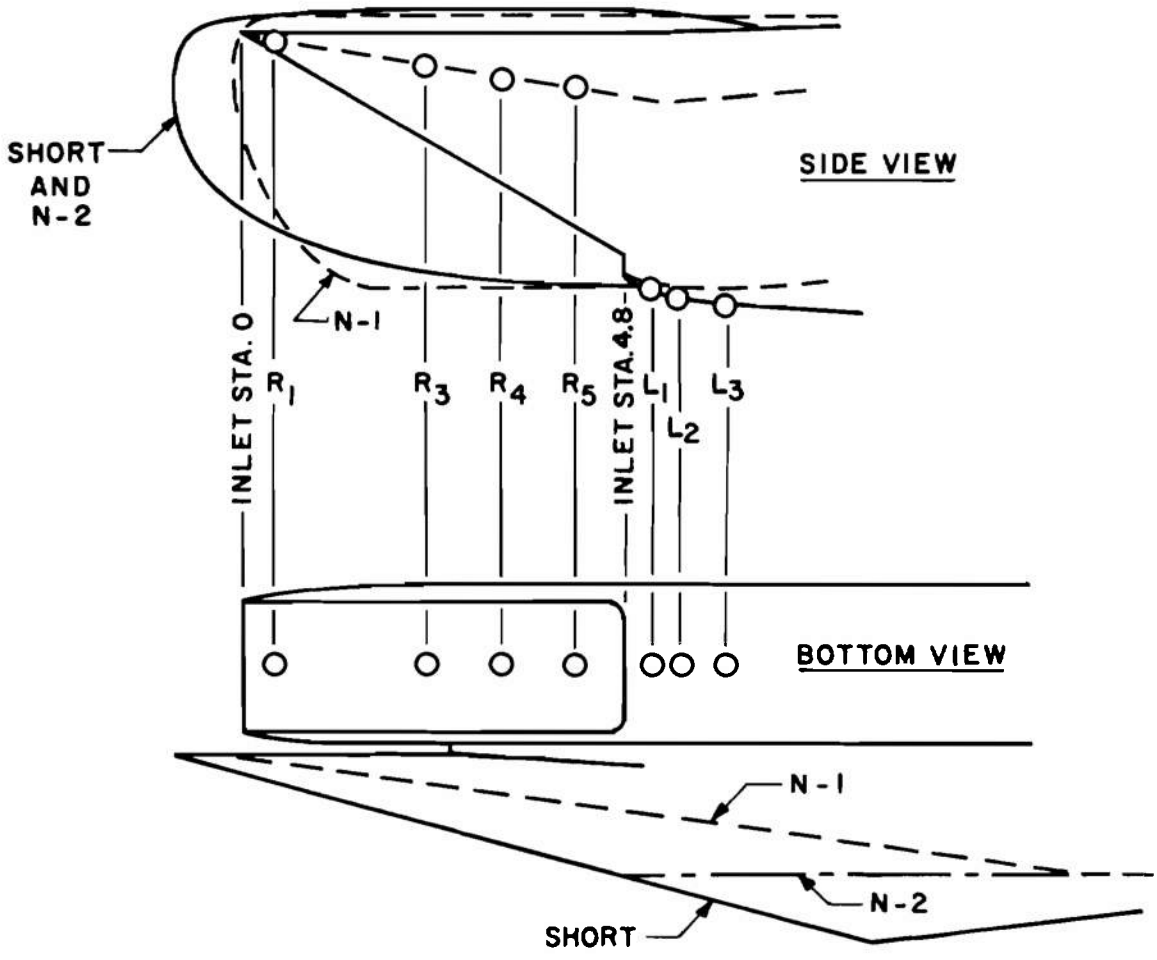

Fig. 10 Inlet Model Configurations and Pressure Orifice Locations

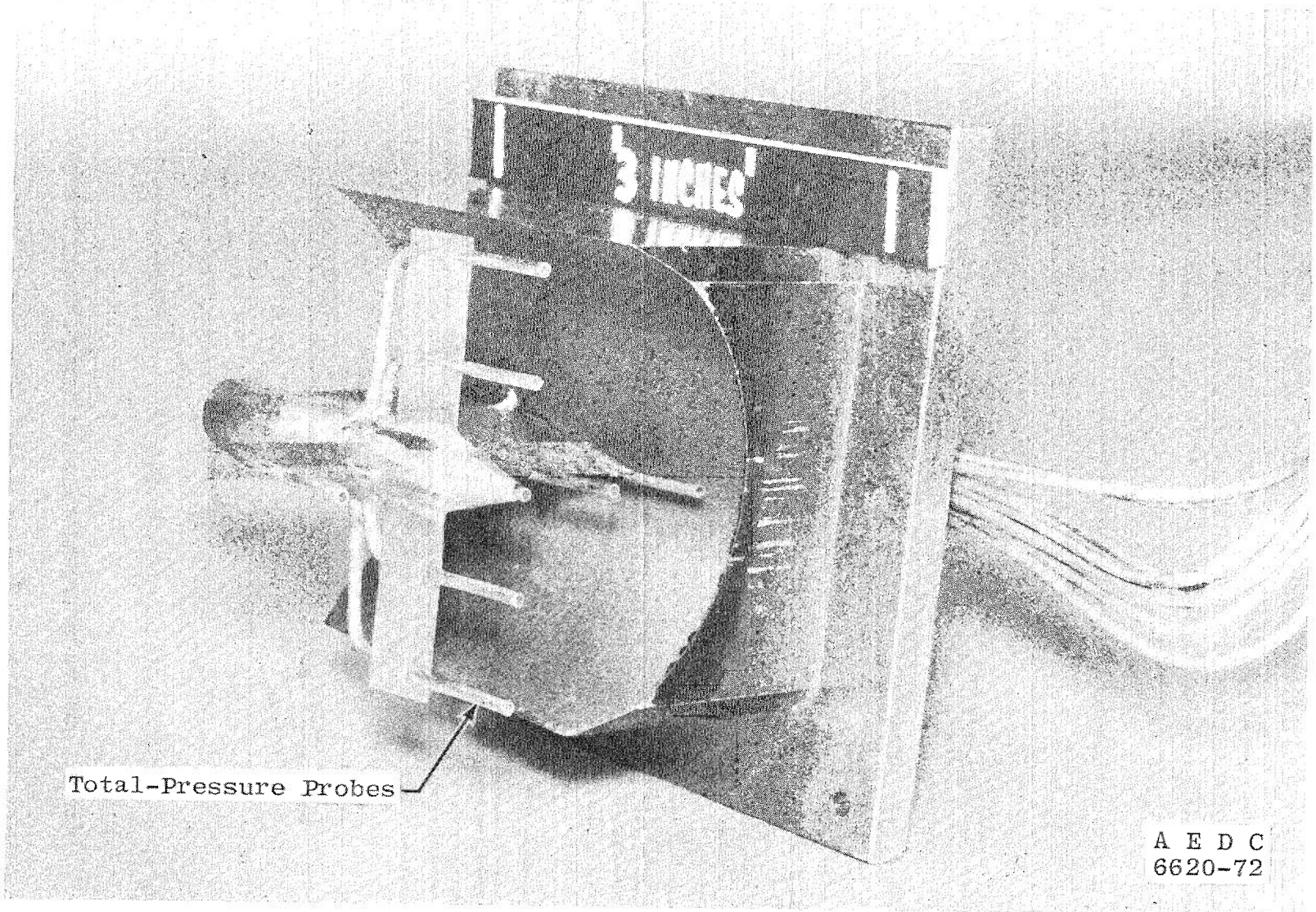

Fig. 11 Engine-Face Station Total-Pressure Rake

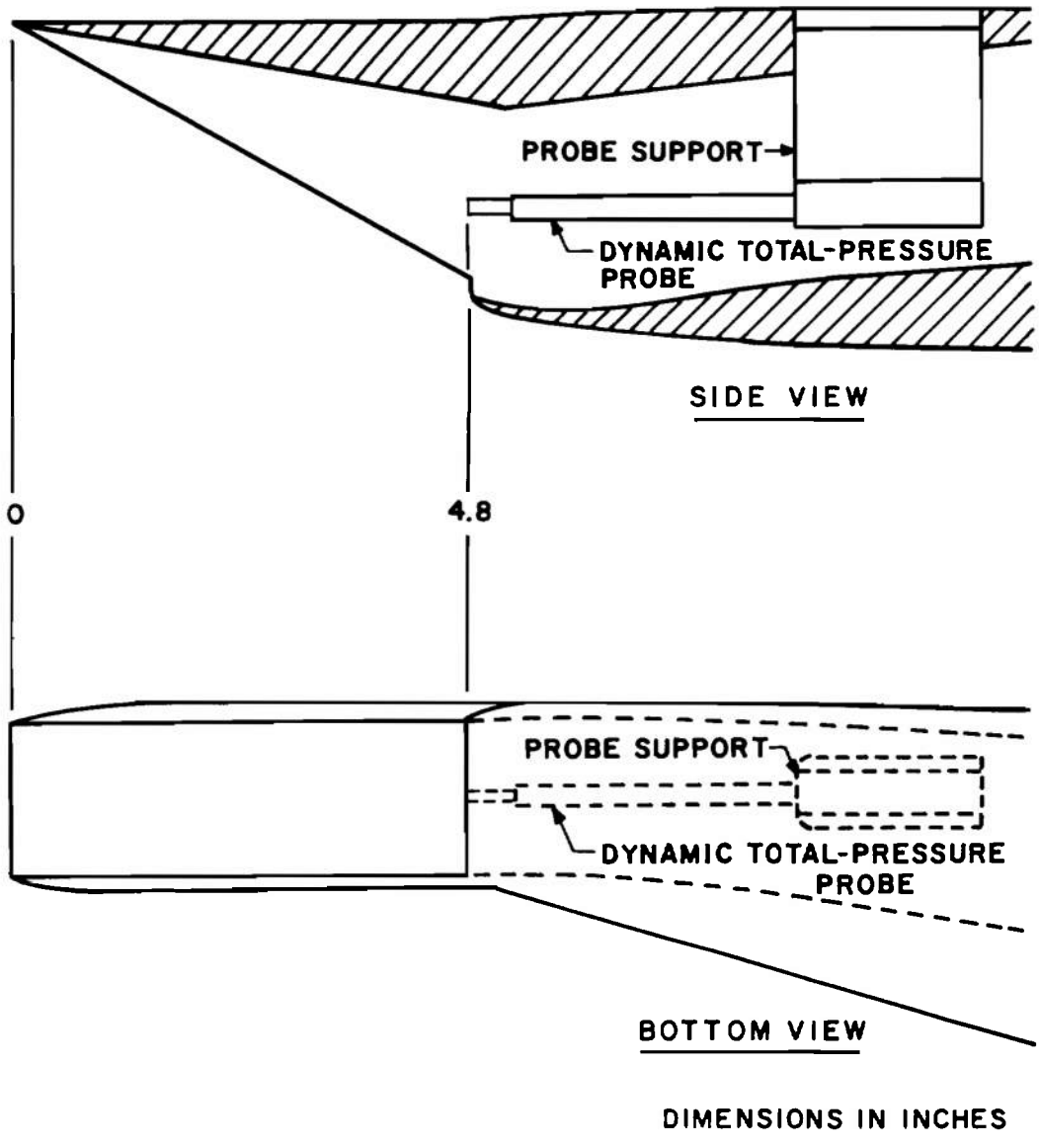

Fig. 12 Schematic of Dynamic Total-Pressure Probe Installation

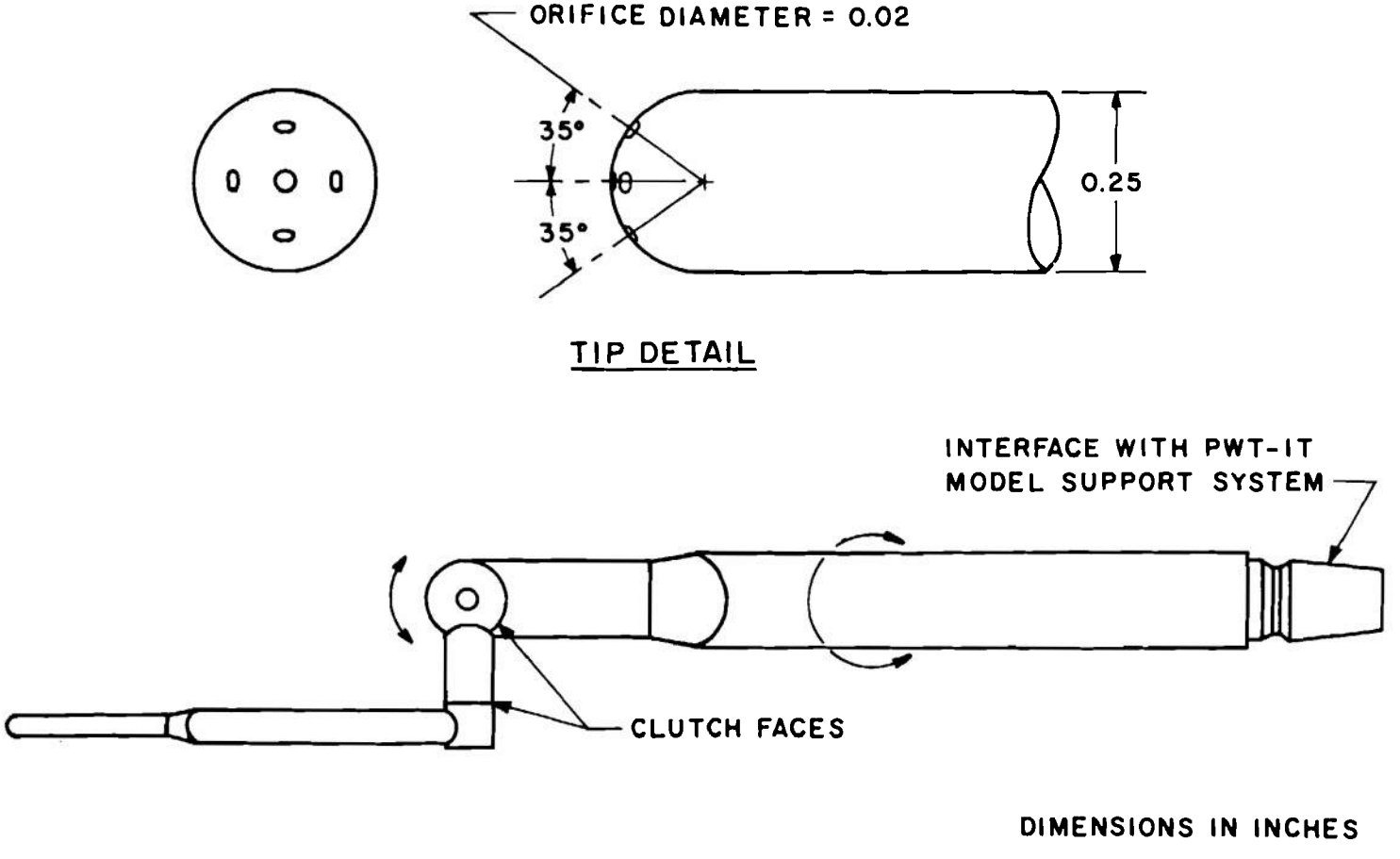

Fig. 13 Flow Angularity Probe and Calibration Support Mechanism

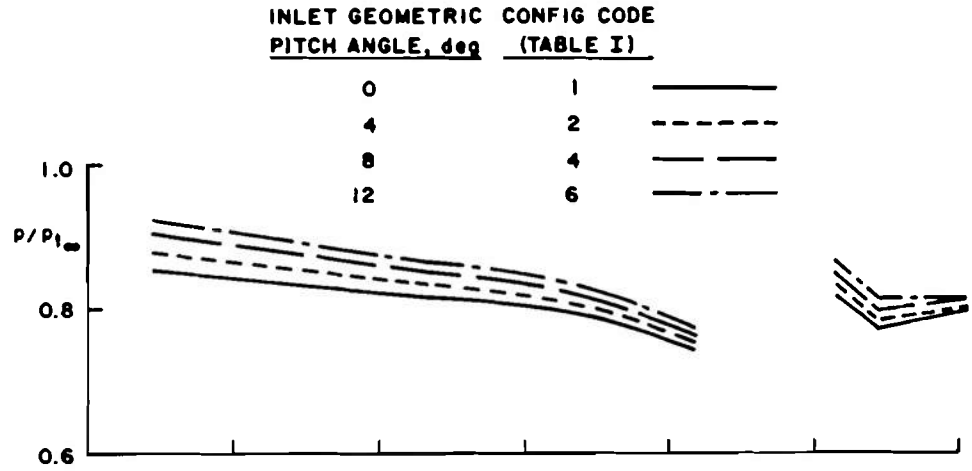

a. $M_\infty = 0.6$

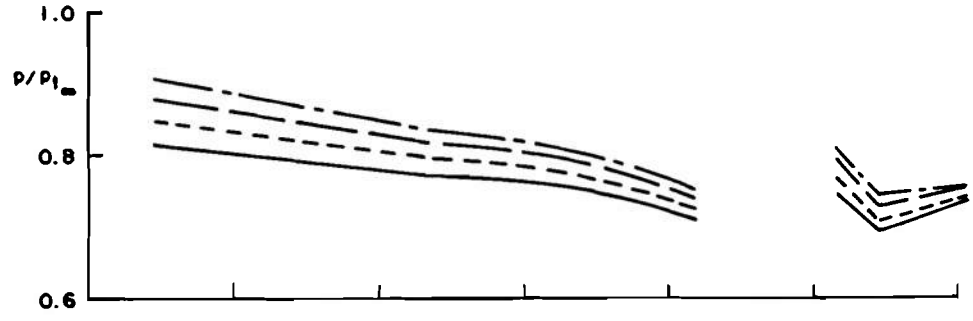

b. $M_\infty = 0.7$

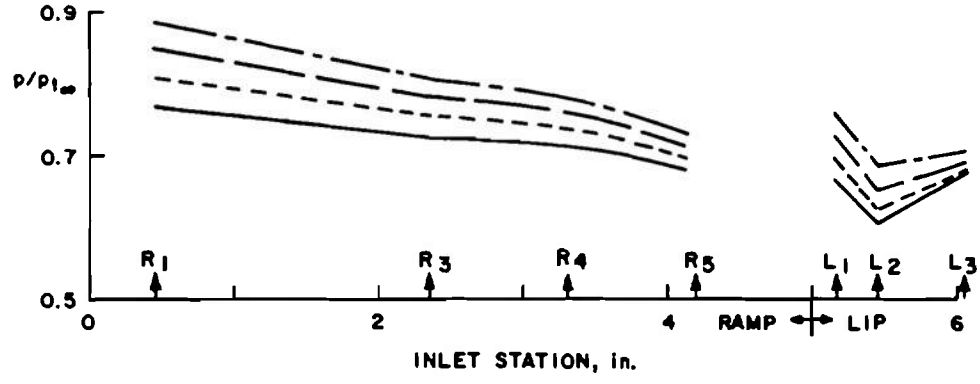

c. $M_\infty = 0.8$

Fig. 14 Inlet Ramp and Lip Pressures for the Basic Inlet Configuration

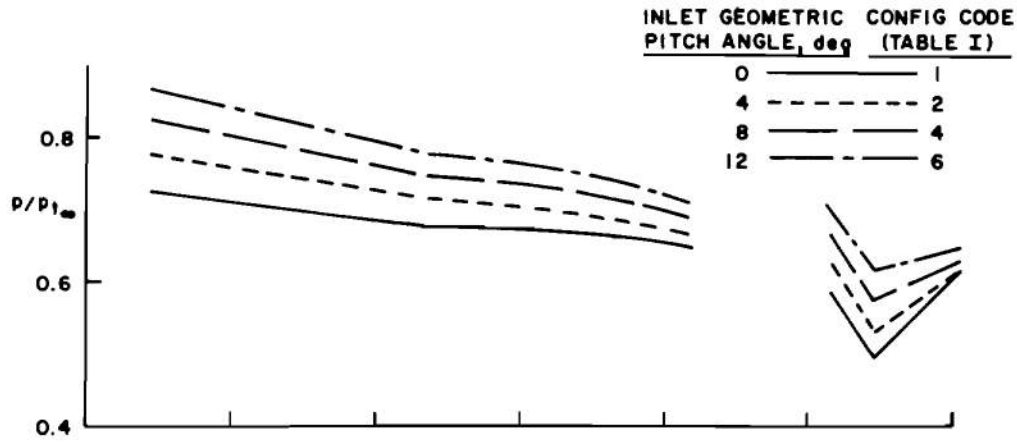

d. $M_\infty = 0.9$

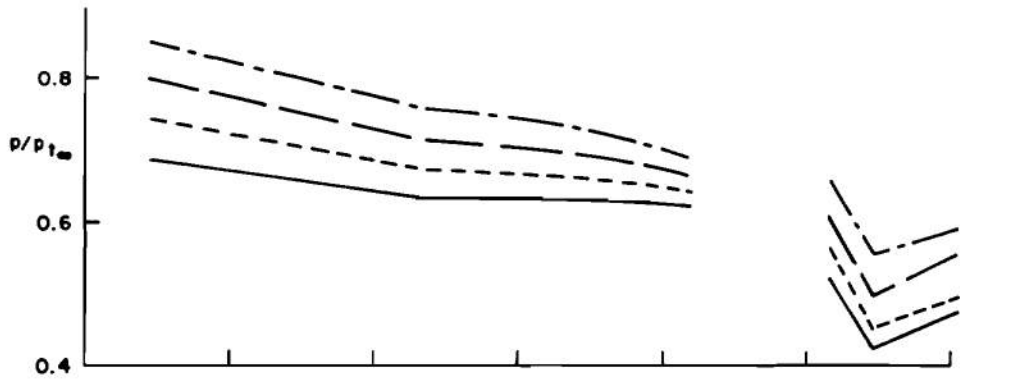

e. $M_\infty = 1.0$

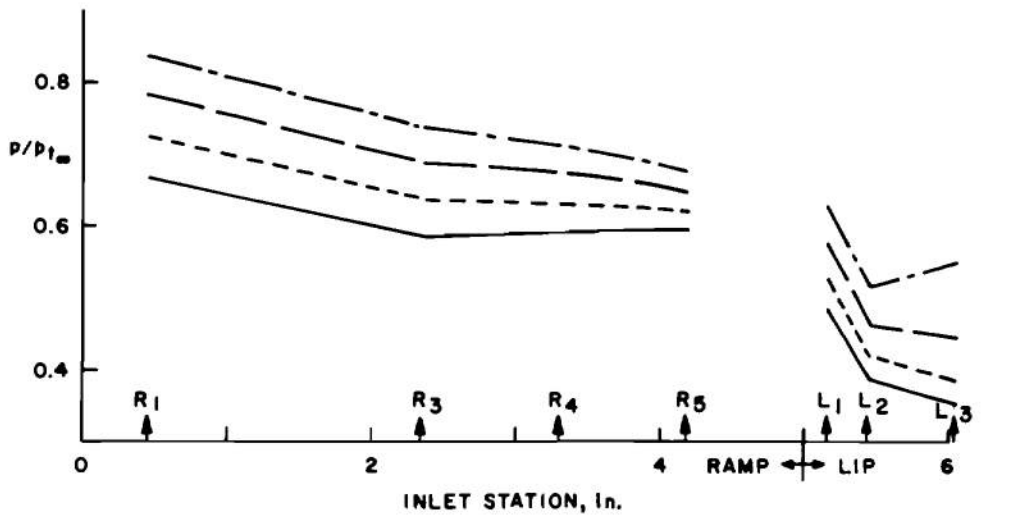

f. $M_\infty = 1.1$

Fig. 14 Concluded

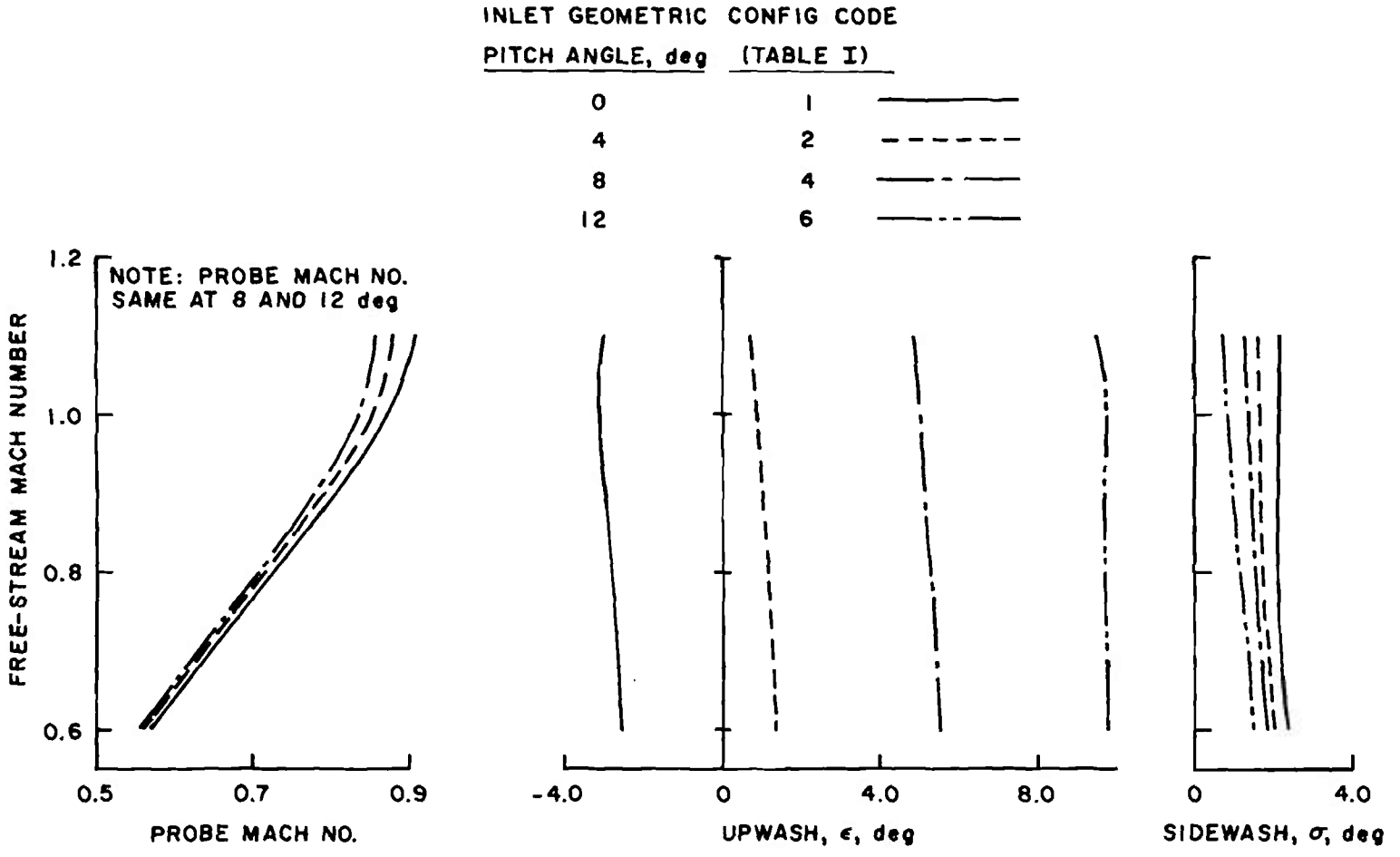

Fig. 15 Flow Angularity Probe Data in Front of the Inlet of the Basic Configuration

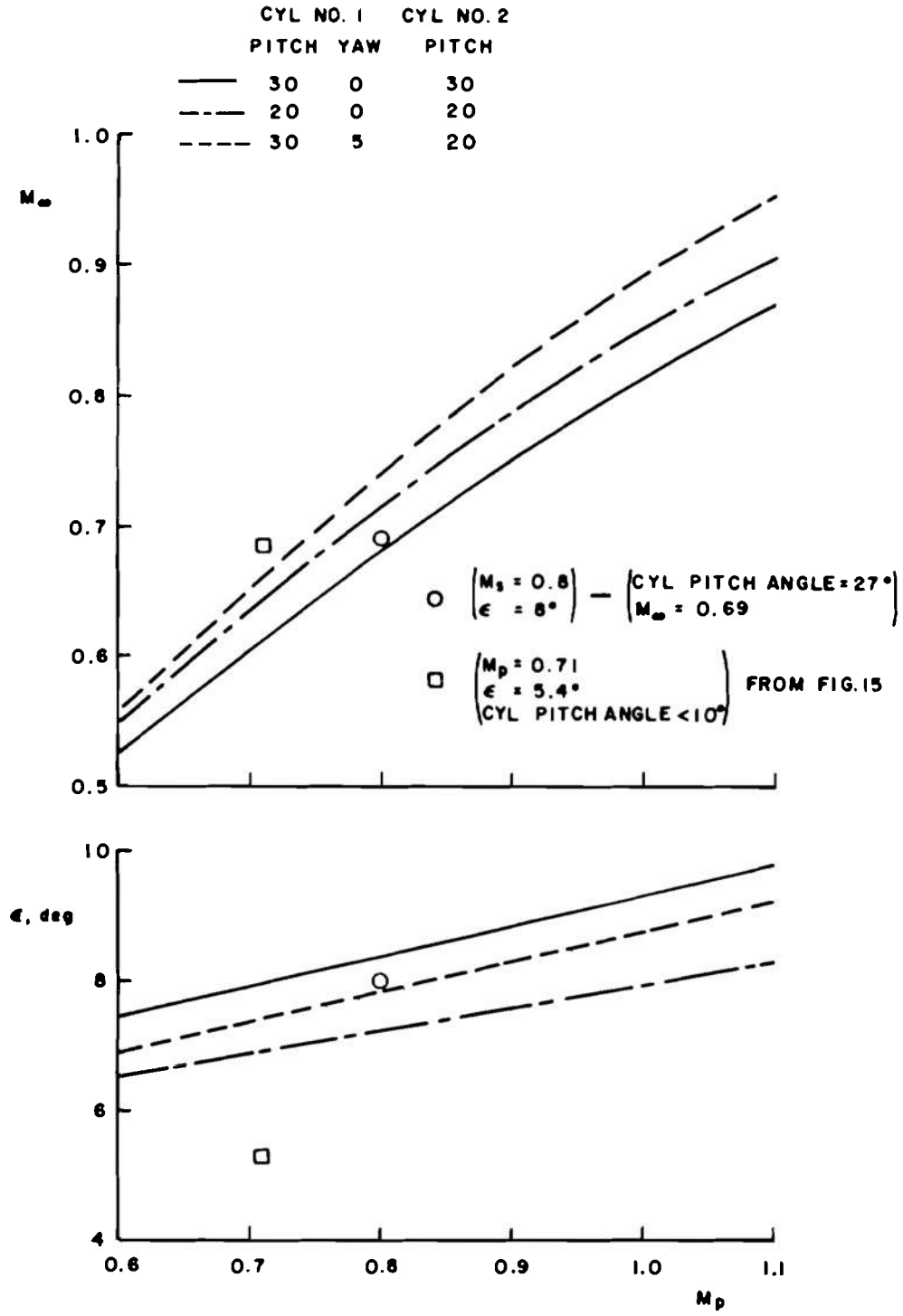

Fig. 16 Free-Stream Mach Number and Upwash Angle versus Flow Angularity Probe Mach Number at Three Cylinder Pitch Angle Settings with the Modified Cylinders Alone

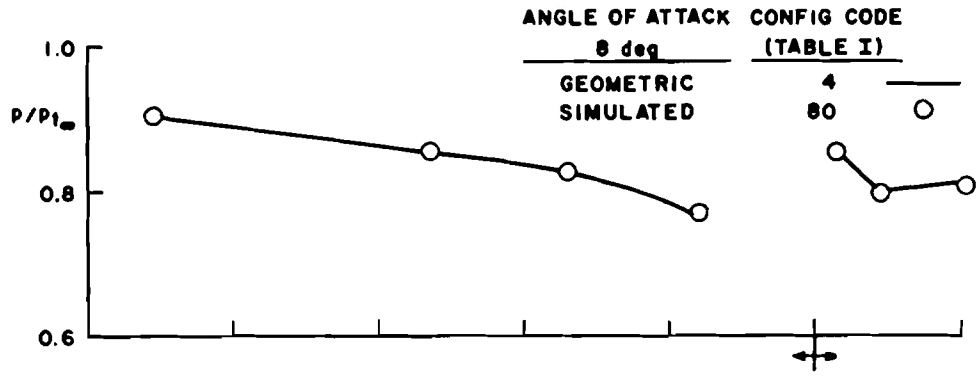

a. $M_\infty = 0.6$

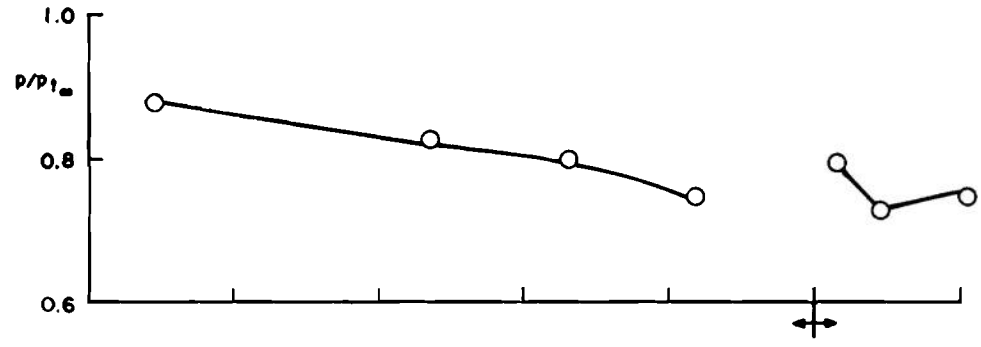

b. $M_\infty = 0.7$

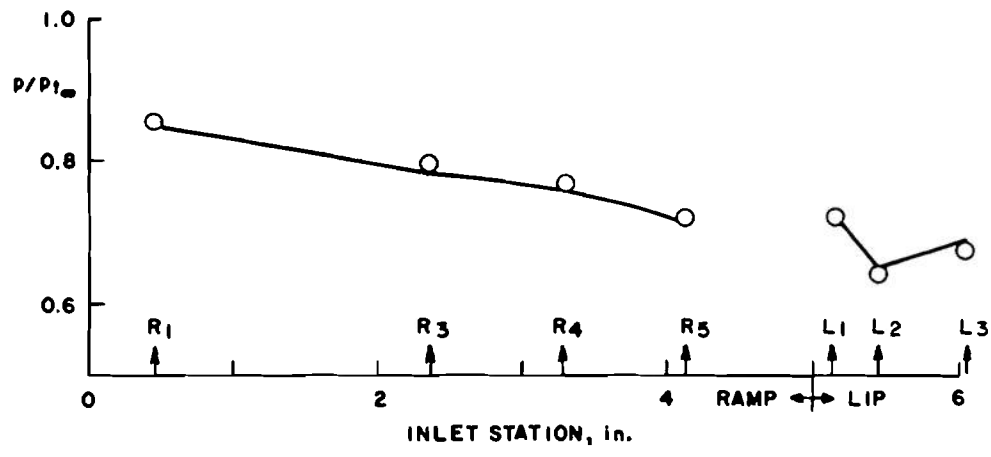

c. $M_\infty = 0.8$

Fig. 17 Comparison of Inlet Ramp and Lip Pressures for 8-deg Simulated and Geometric Pitch

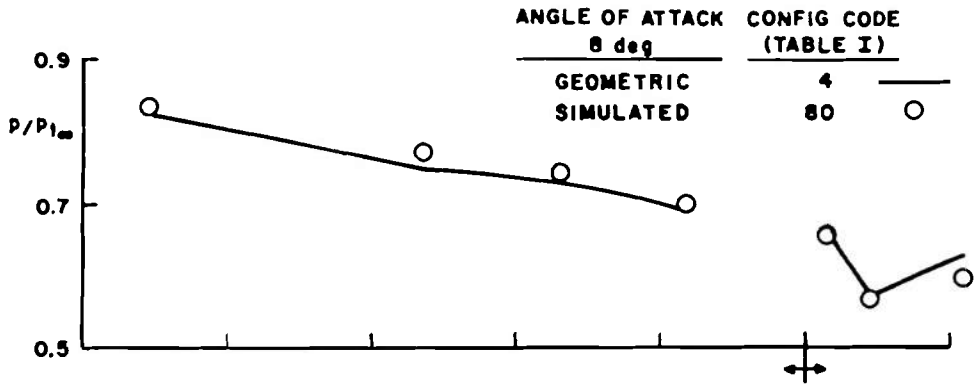

d. $M_\infty = 0.9$

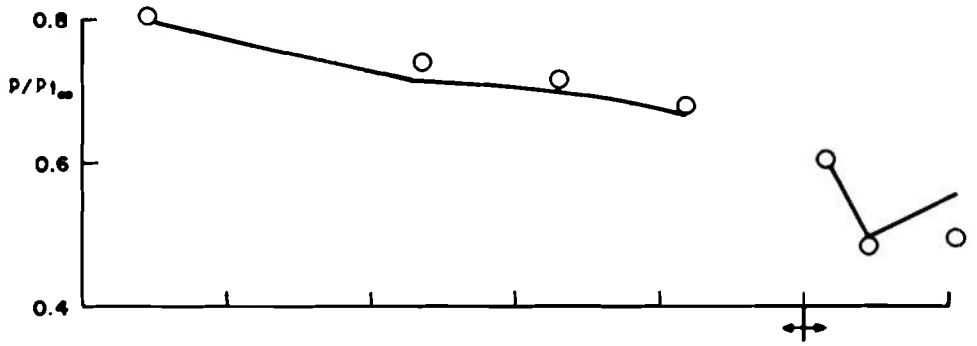

e. $M_\infty = 1.0$

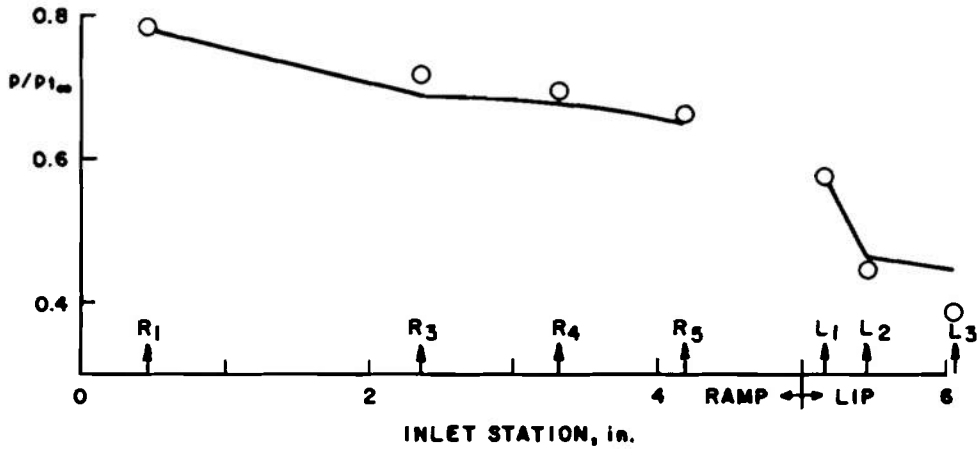

f. $M_\infty = 1.1$

Fig. 17 Concluded

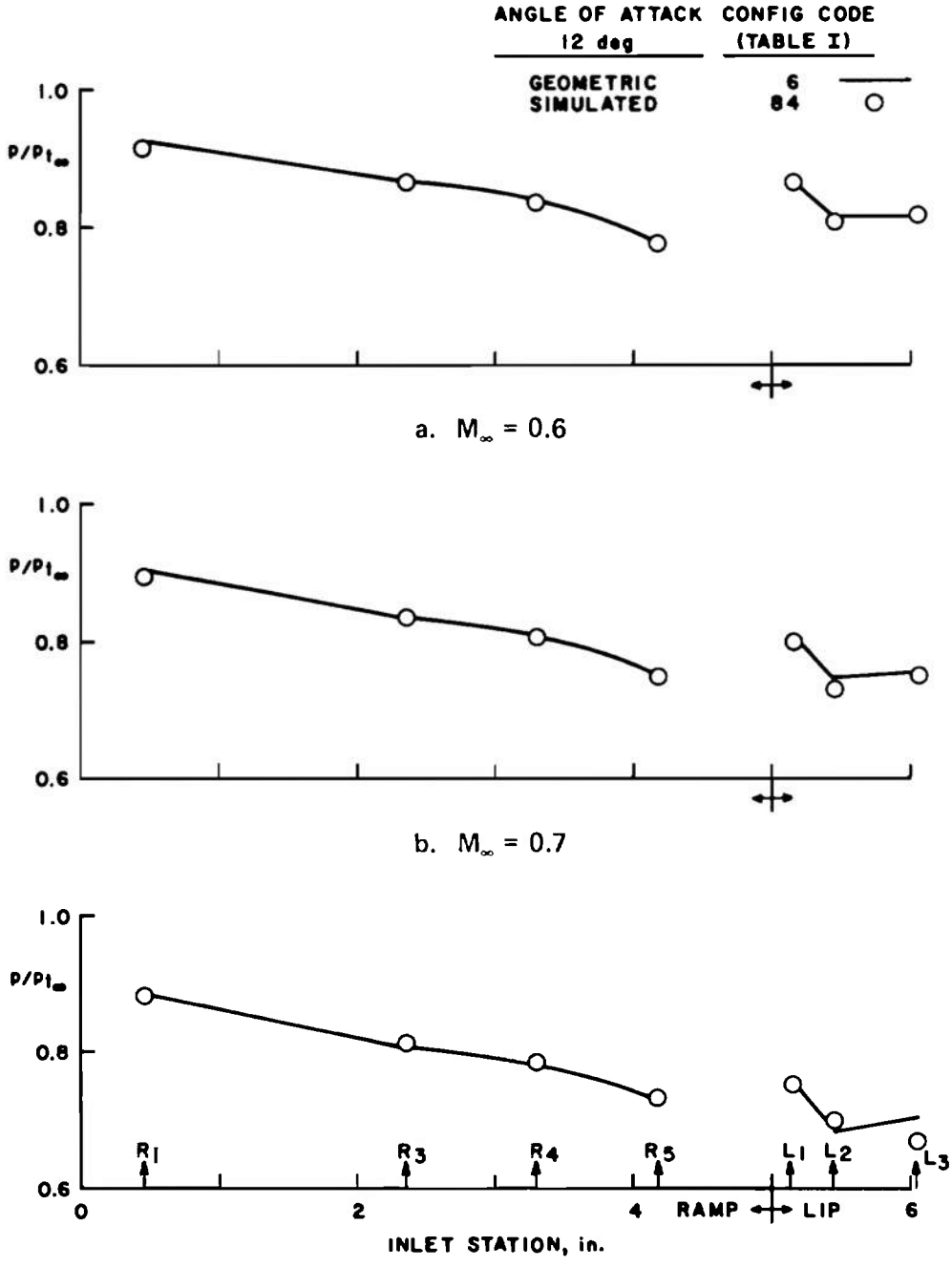

a. $M_\infty = 0.6$

b. $M_\infty = 0.7$

c. $M_\infty = 0.8$

Fig. 18 Comparison of Inlet Ramp and Lip Pressures for 12-deg Simulated and Geometric Pitch

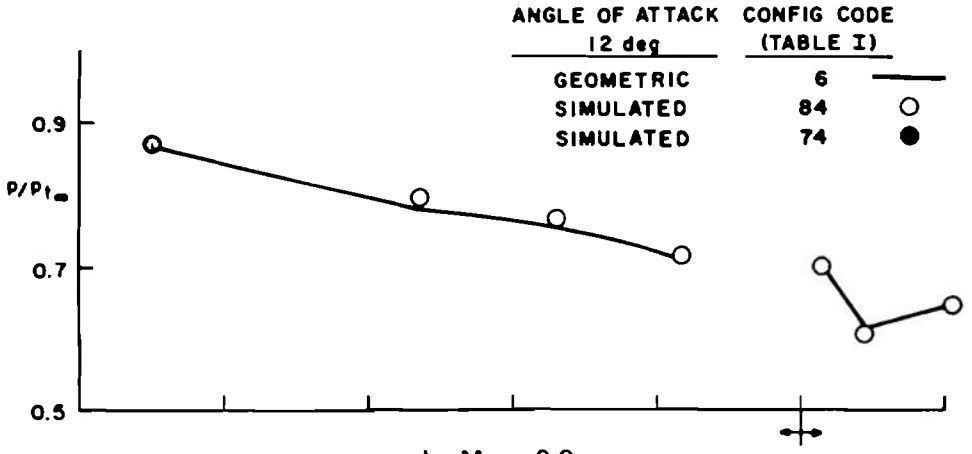

d. $M_\infty = 0.9$

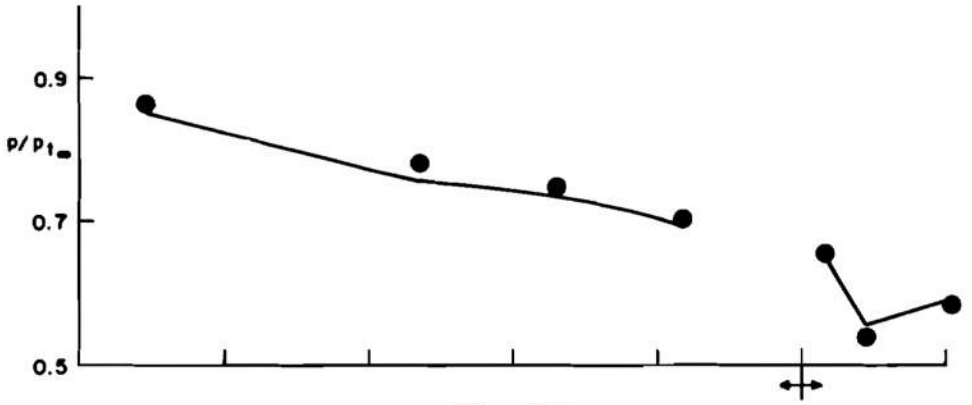

e. $M_\infty = 1.0$

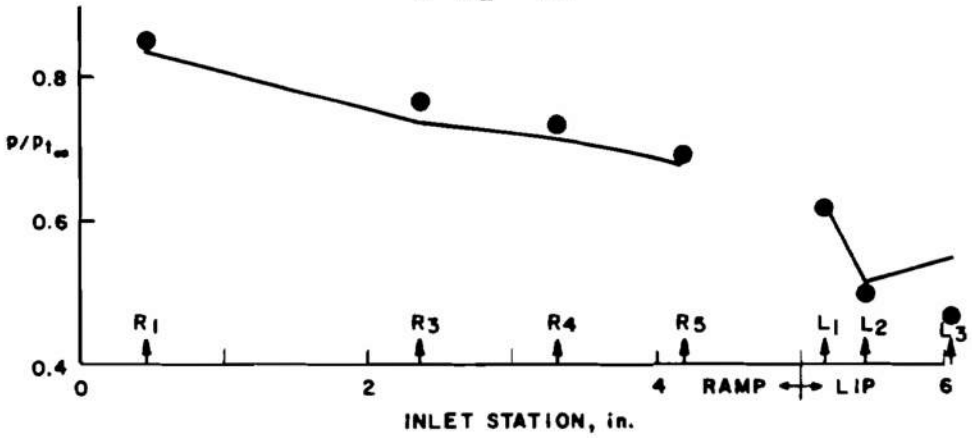

f. $M_\infty = 1.1$

Fig. 18 Concluded

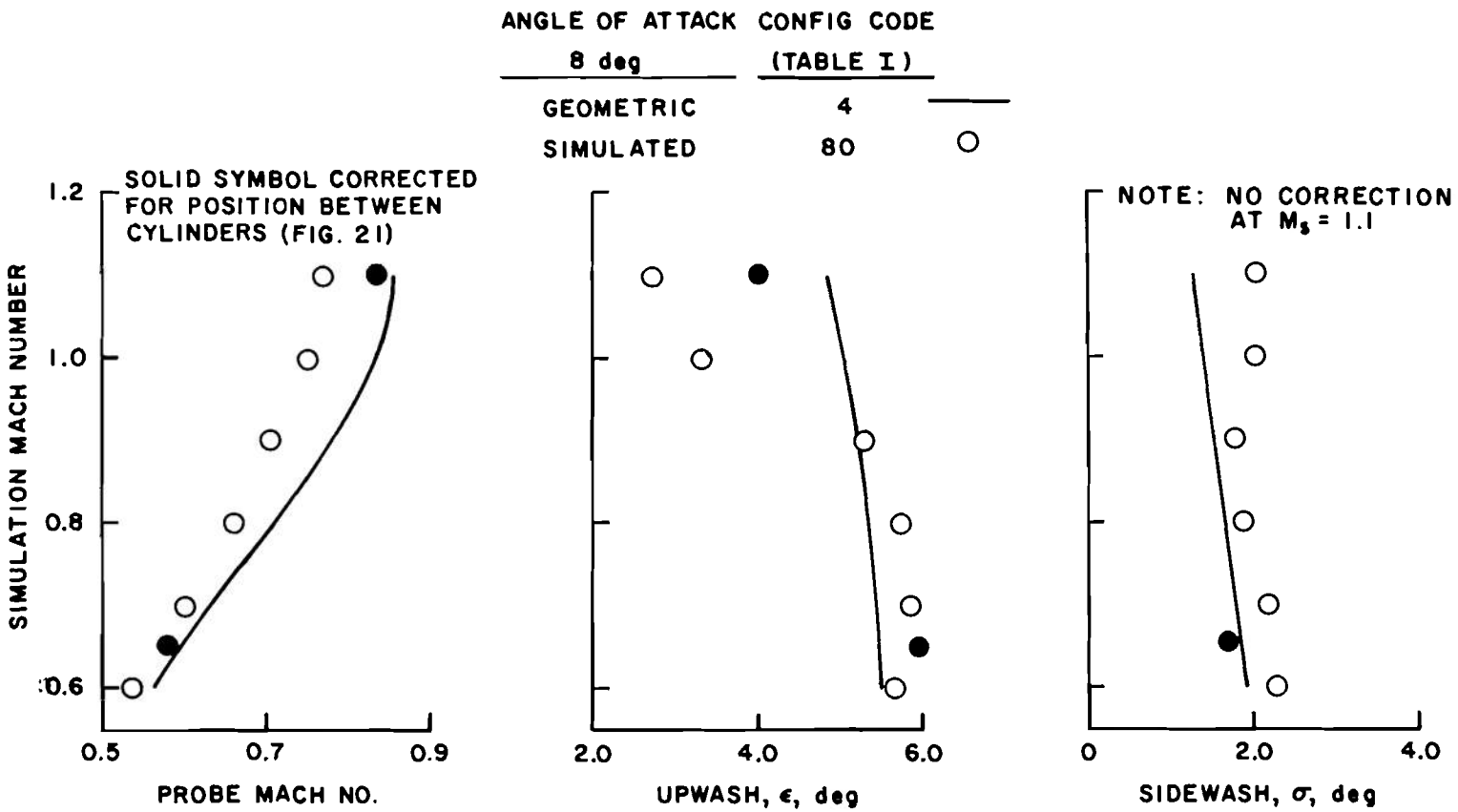

Fig. 19 Comparison of Flow Angularity Probe Data in Front of the Inlet for 8-deg Simulated and Geometric Pitch

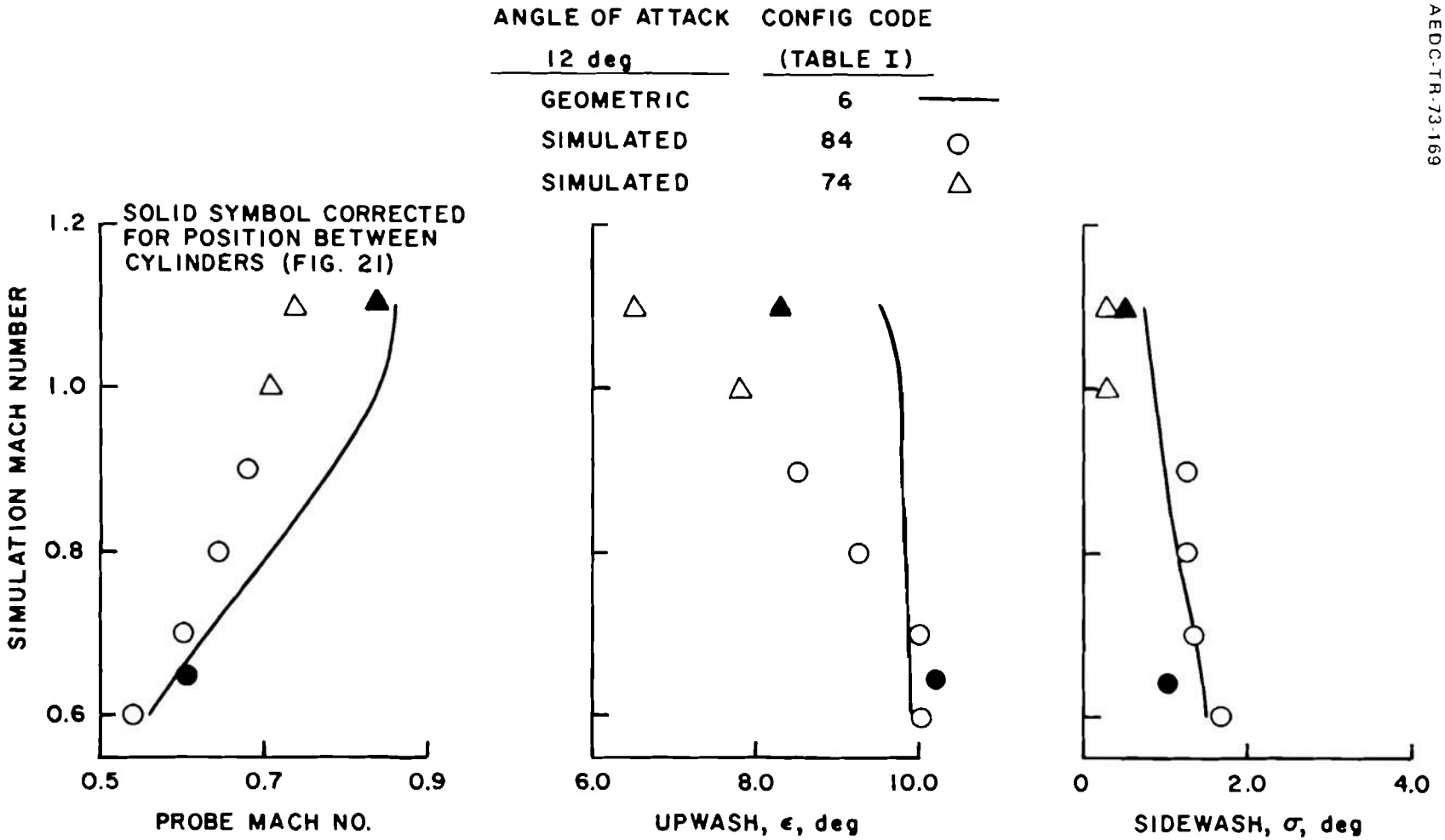

Fig. 20 Comparison of Flow Angularity Probe Data in Front of the Inlet for 12-deg Simulated and Geometric Pitch

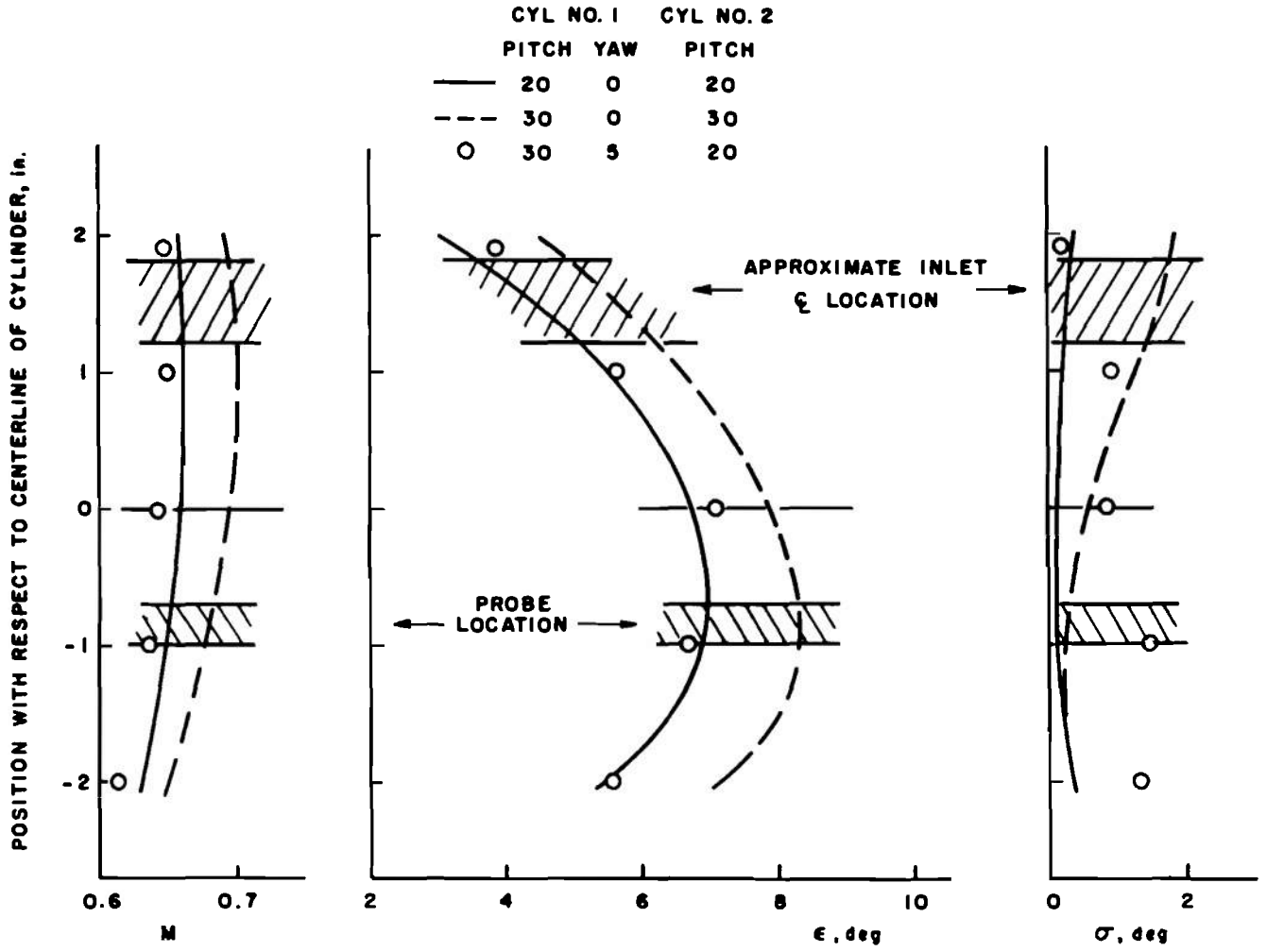

a. Free-Stream Mach Number 0.6

Fig. 21 Variation in Local Mach Number, Upwash Angle, and Sidewash Angle with Position Between the Modified Cylinder Flow-Shaping Devices

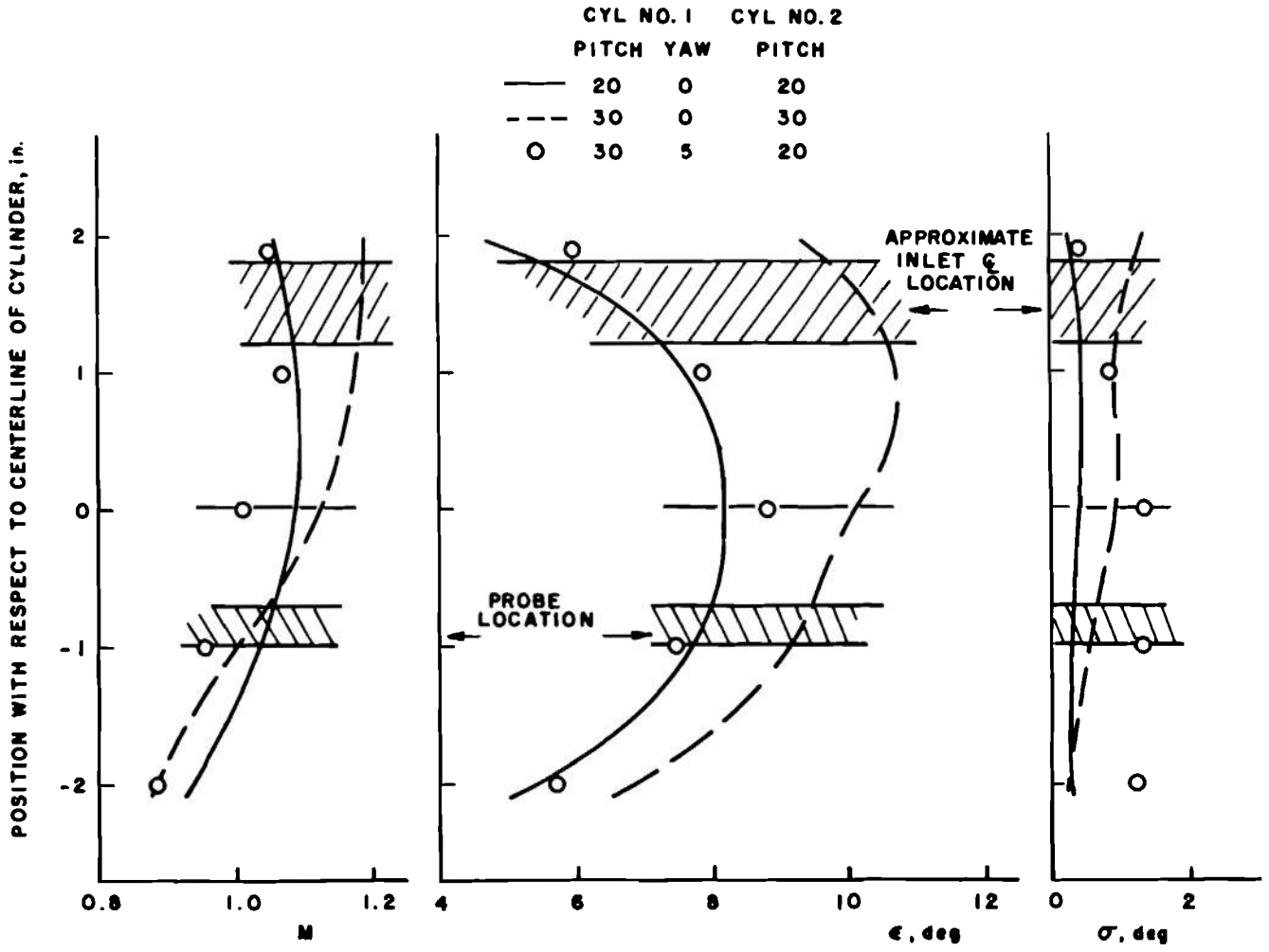

b. Free-Stream Mach Number 0.9

Fig. 21 Concluded

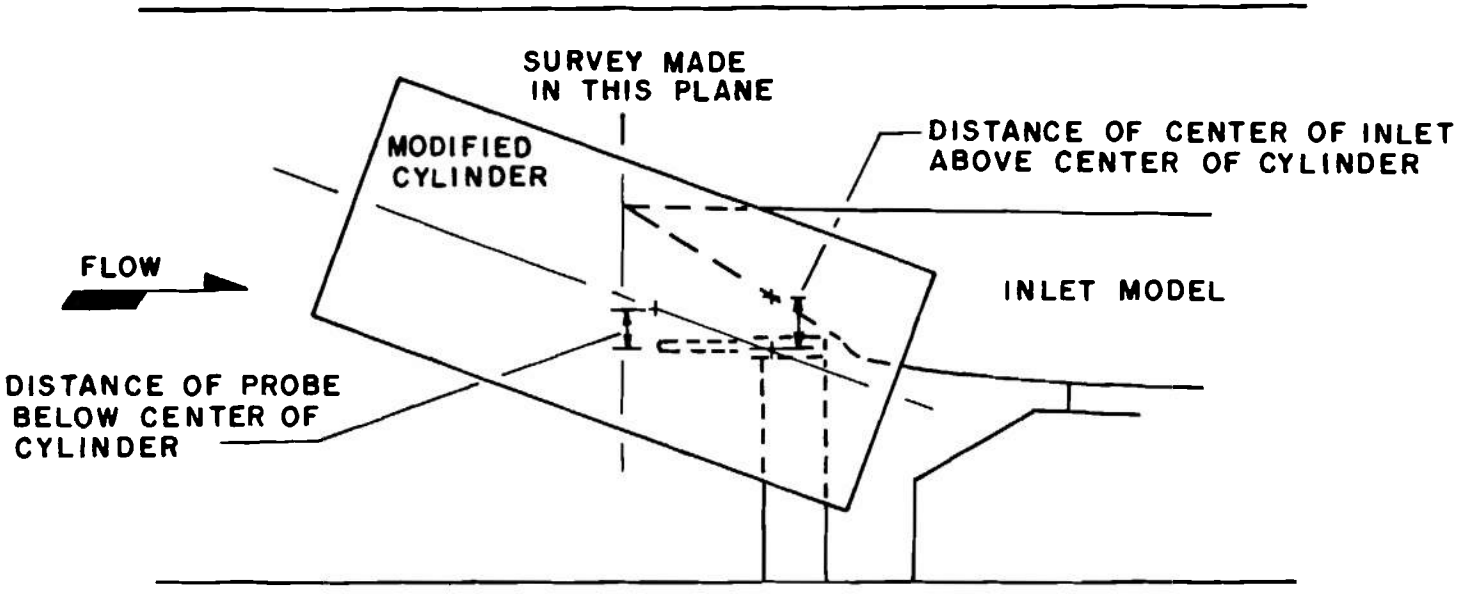

Fig. 22 Sketch Showing the Position of the Probe Tip and Inlet Center Relative to the Center of the Modified Cylinders

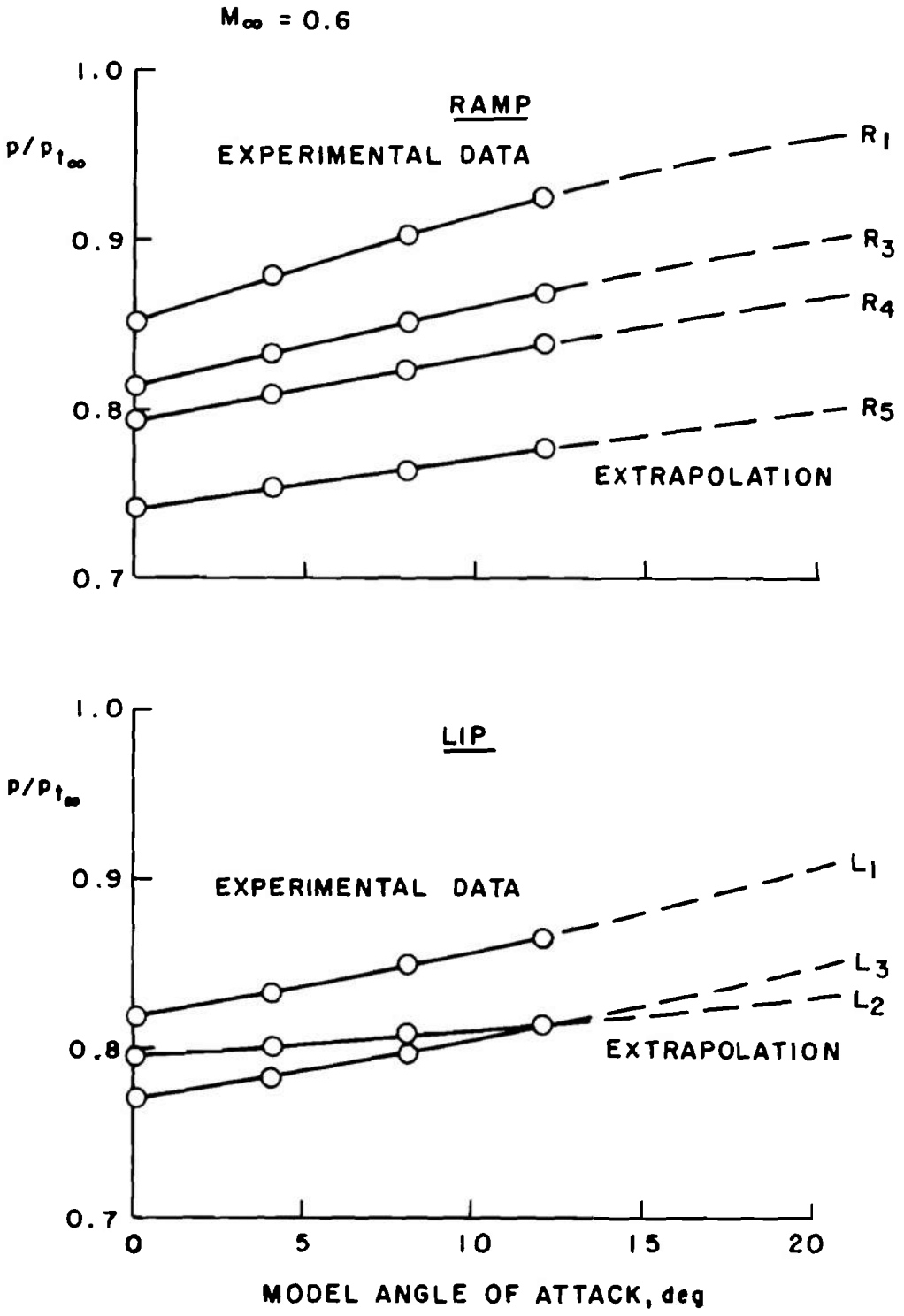

Fig. 23 Typical Extrapolation of Ramp and Lip Pressure Distribution Data to Higher Angles of Attack for the Basic Inlet Configuration

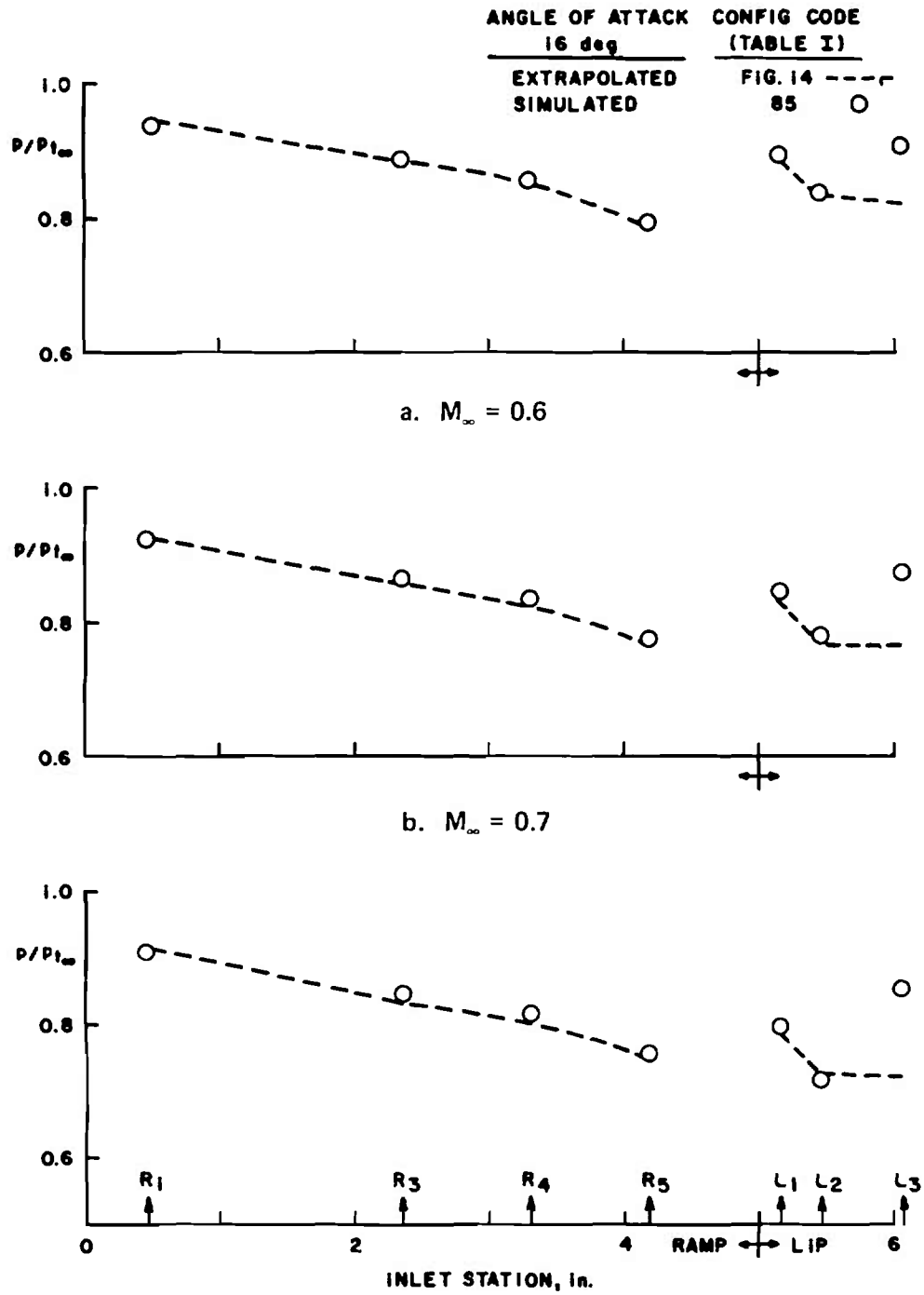

Fig. 24 Comparison of Inlet Ramp and Lip Pressures for 16-deg Simulated and Geometric Pitch

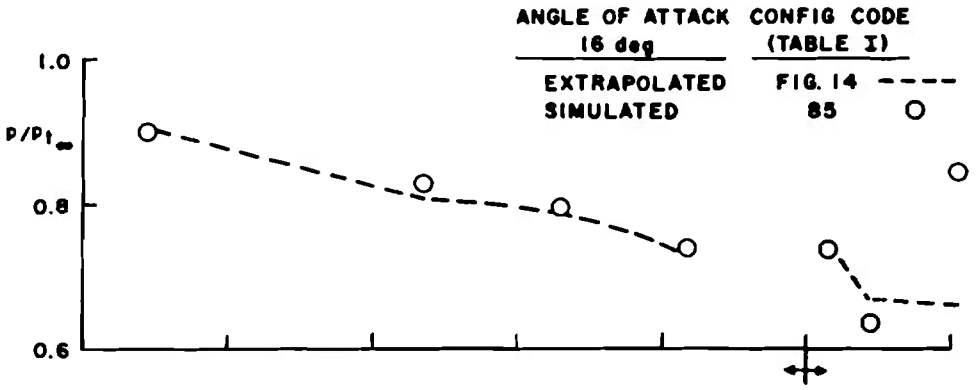

d. $M_\infty = 0.9$

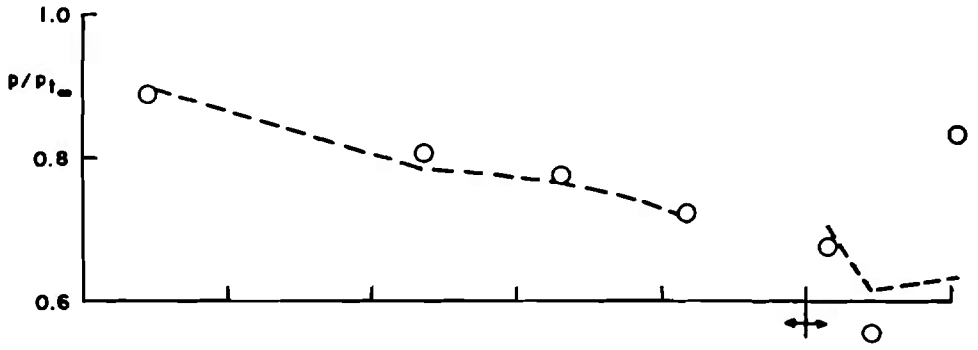

e. $M_\infty = 1.0$

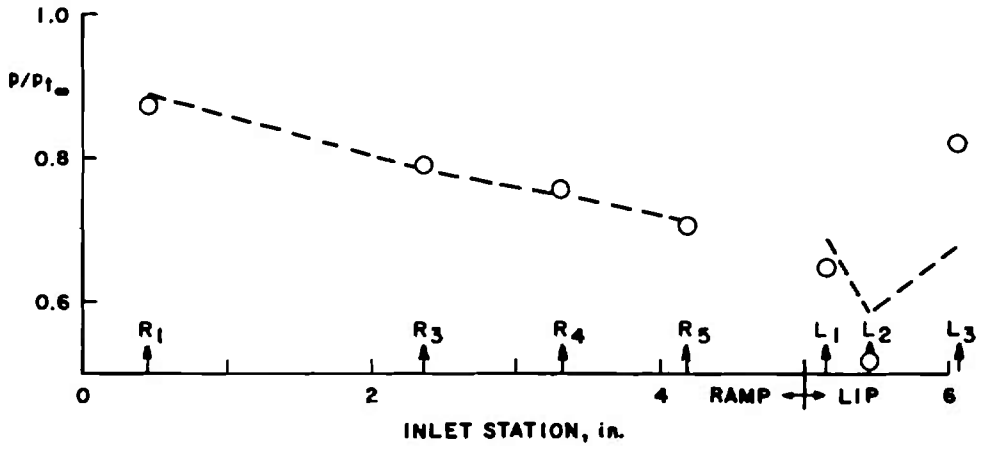

f. $M_\infty = 1.1$

Fig. 24 Concluded

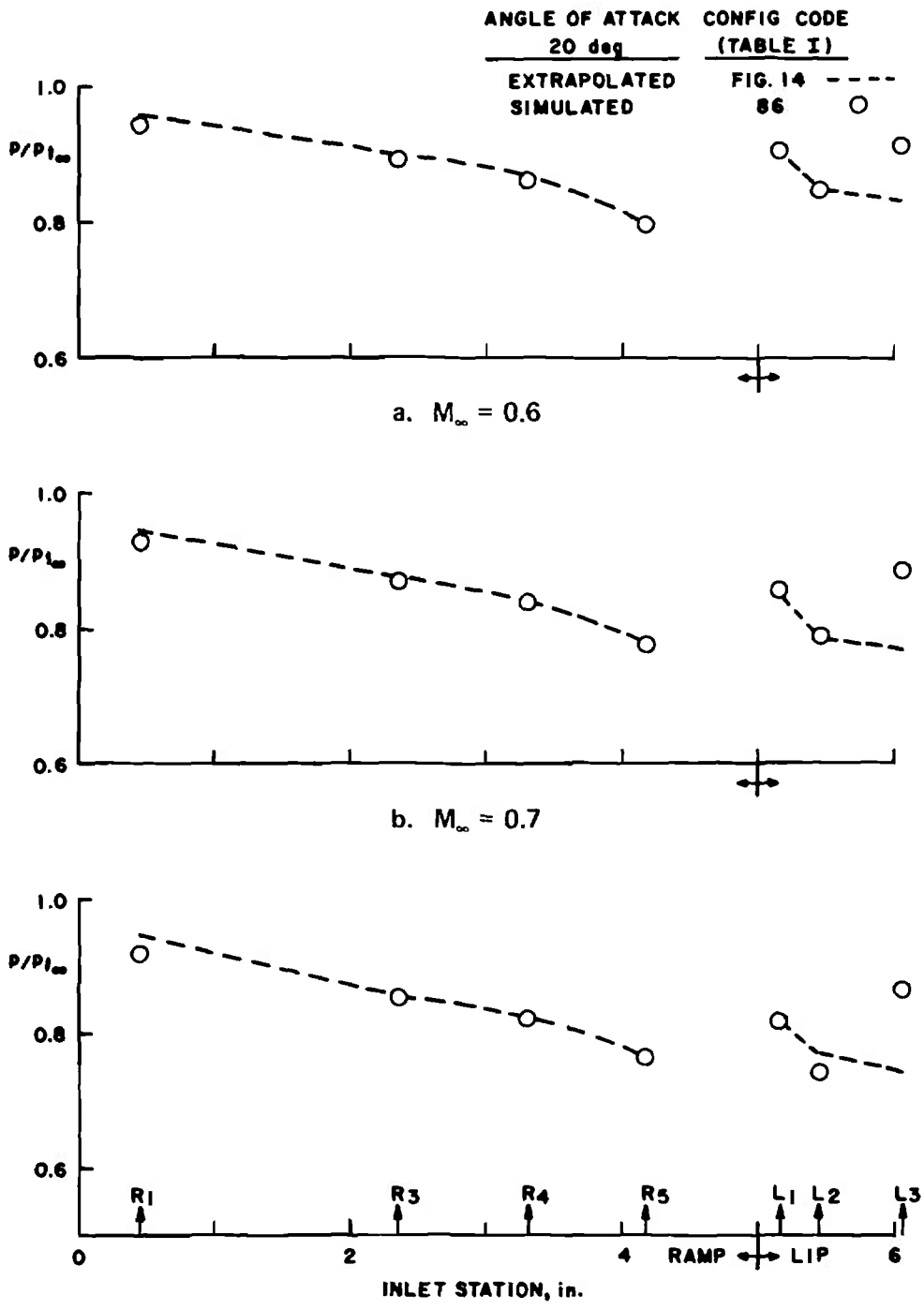

a. $M_\infty = 0.6$

b. $M_\infty = 0.7$

c. $M_\infty = 0.8$

Fig. 25 Comparison of Inlet Ramp and Lip Pressures for 20-deg Simulated and Geometric Pitch

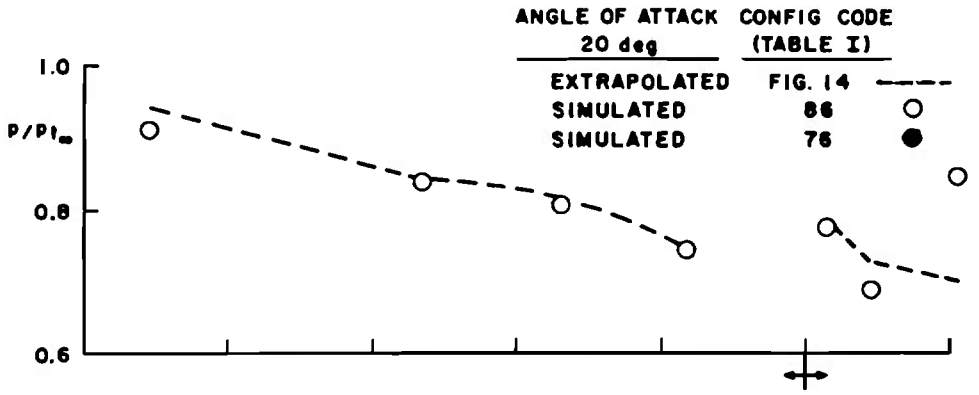

d. $M_\infty = 0.9$

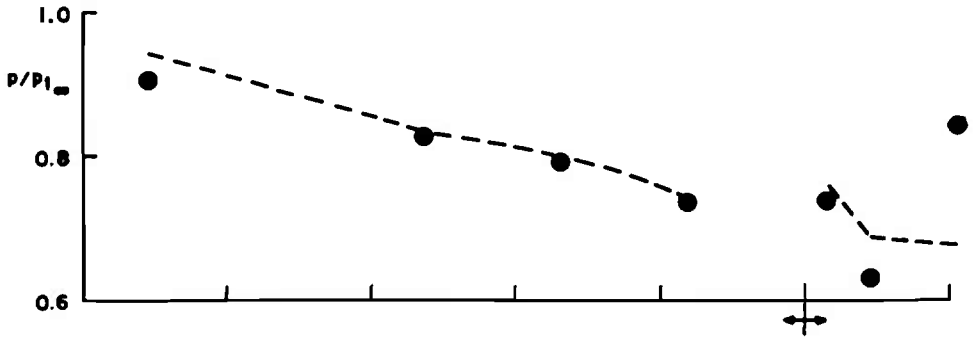

e. $M_\infty = 1.0$

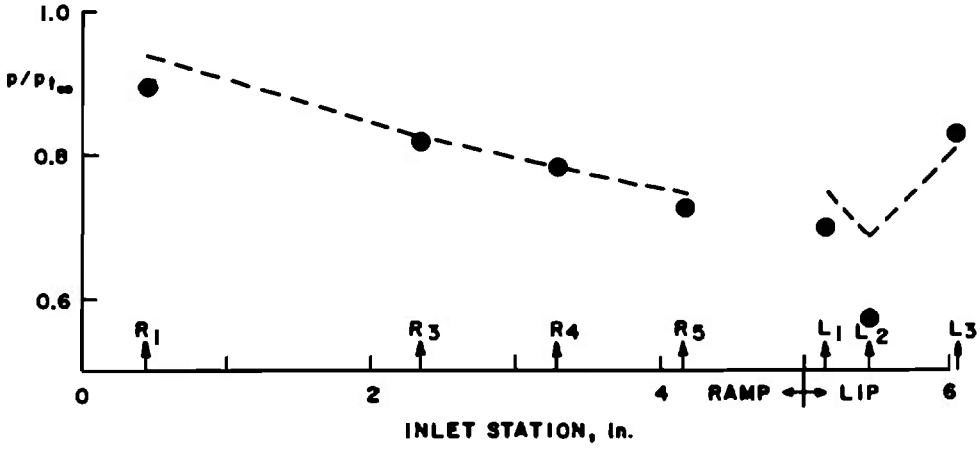

f. $M_\infty = 1.1$

Fig. 25 Concluded

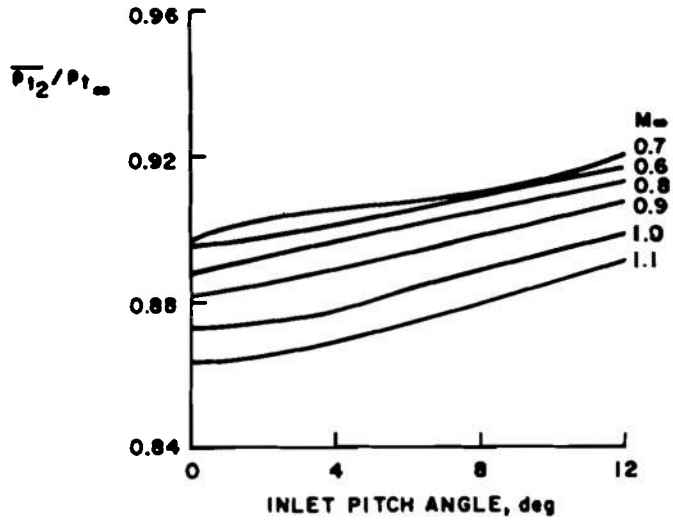

Fig. 26 Variation in Average Total Pressure at the Engine-Face Station with Mach Number for the Basic Inlet Configuration

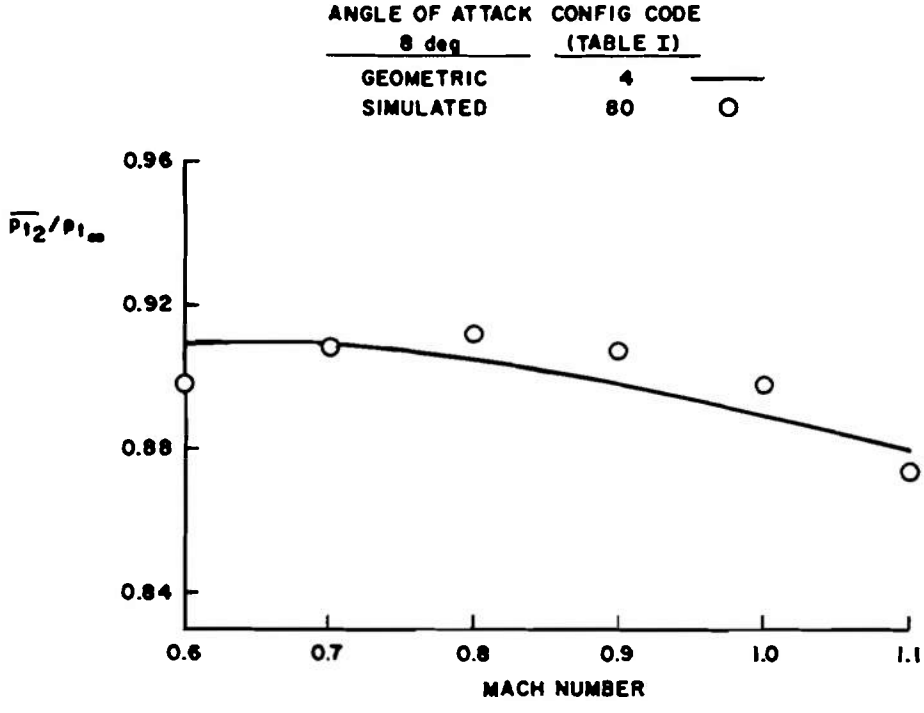

Fig. 27 Comparison of the Average Total Pressure at the Engine-Face Station for 8-deg Simulated and Geometric Pitch

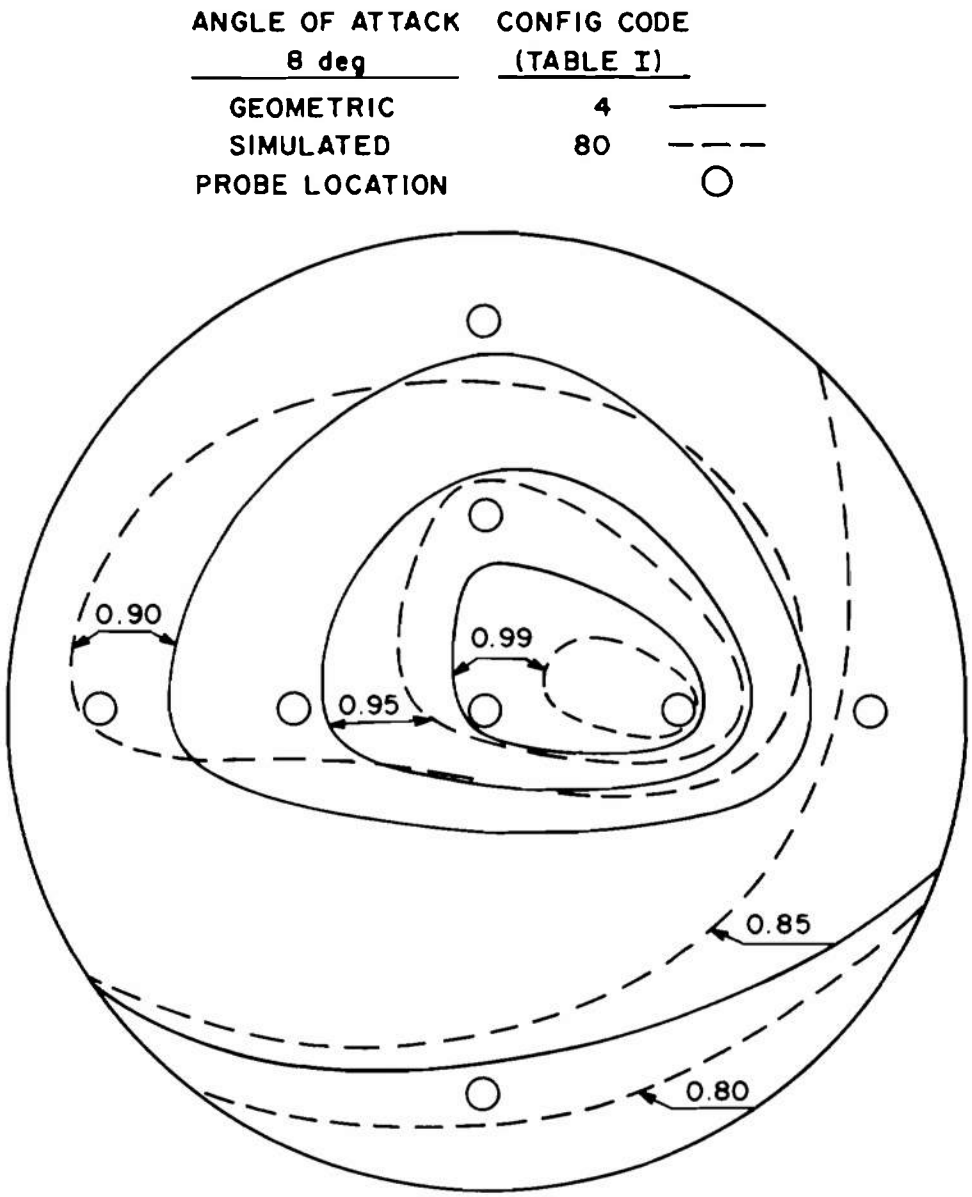

a. $M_\infty = 0.6$

Fig. 28 Engine-Face Maps for 8-deg Simulated and Geometric Pitch ($p_{t_E}/p_{t_{E_{MAX}}}$)

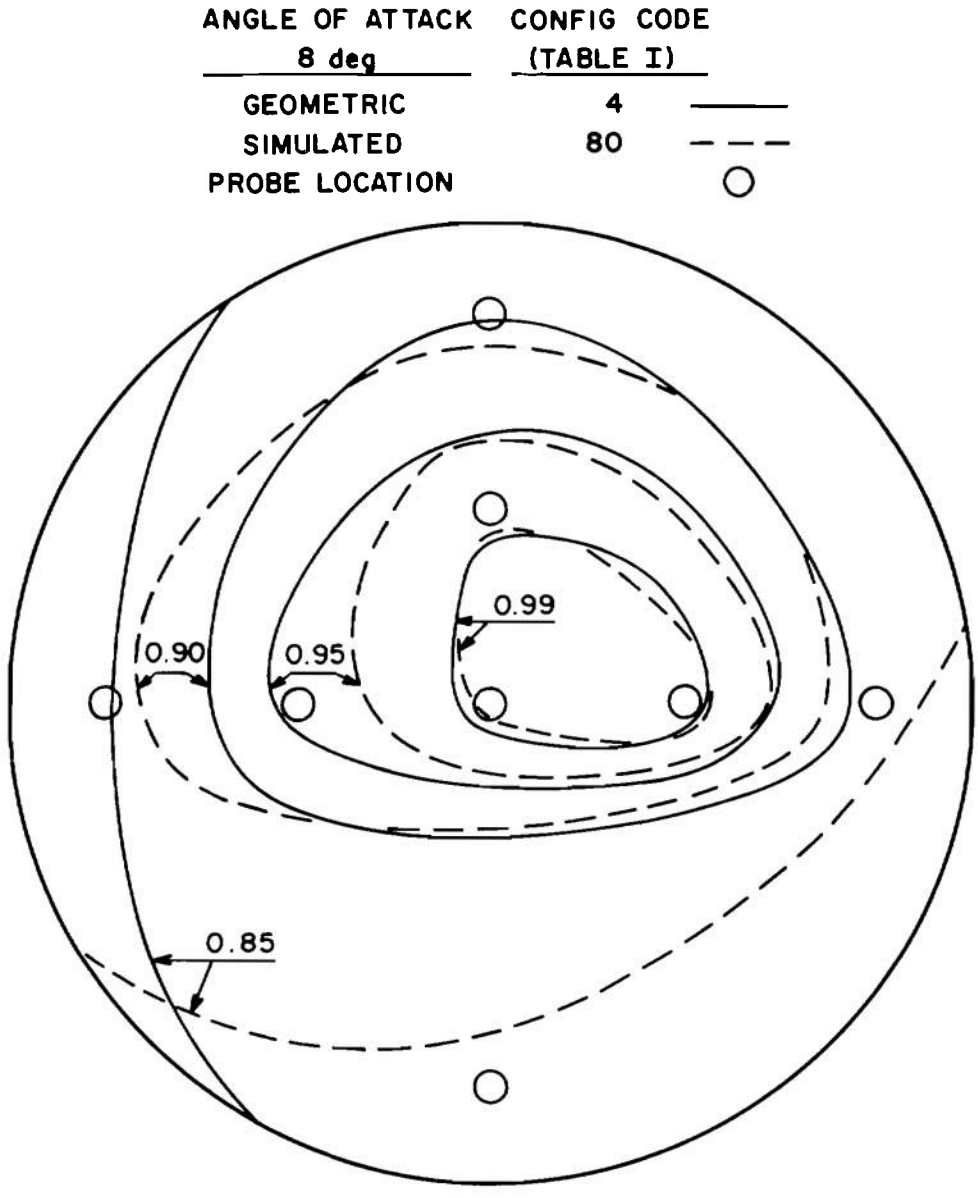

b. $M_\infty = 0.7$
Fig. 28 Continued

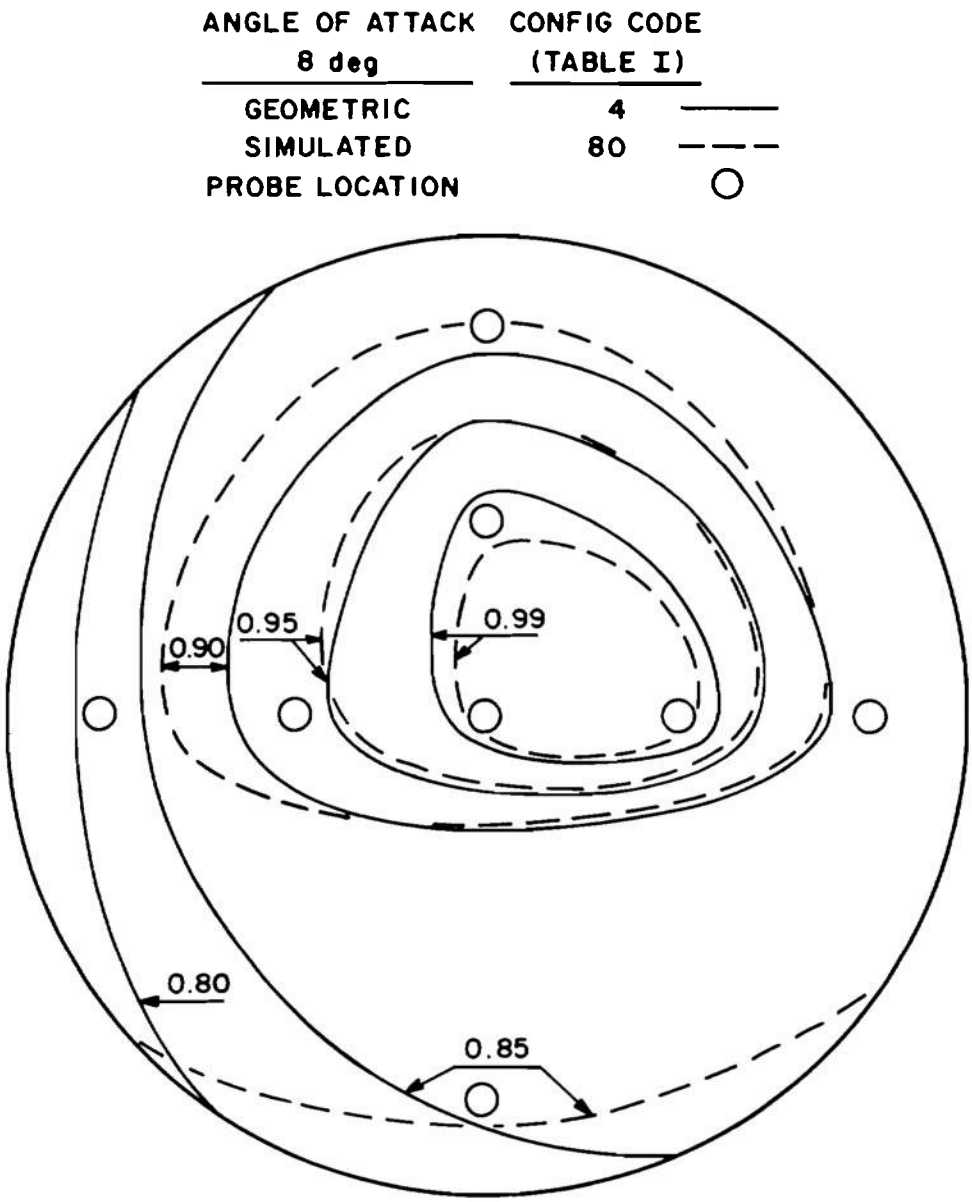

c. $M_\infty = 0.8$
Fig. 28 Continued

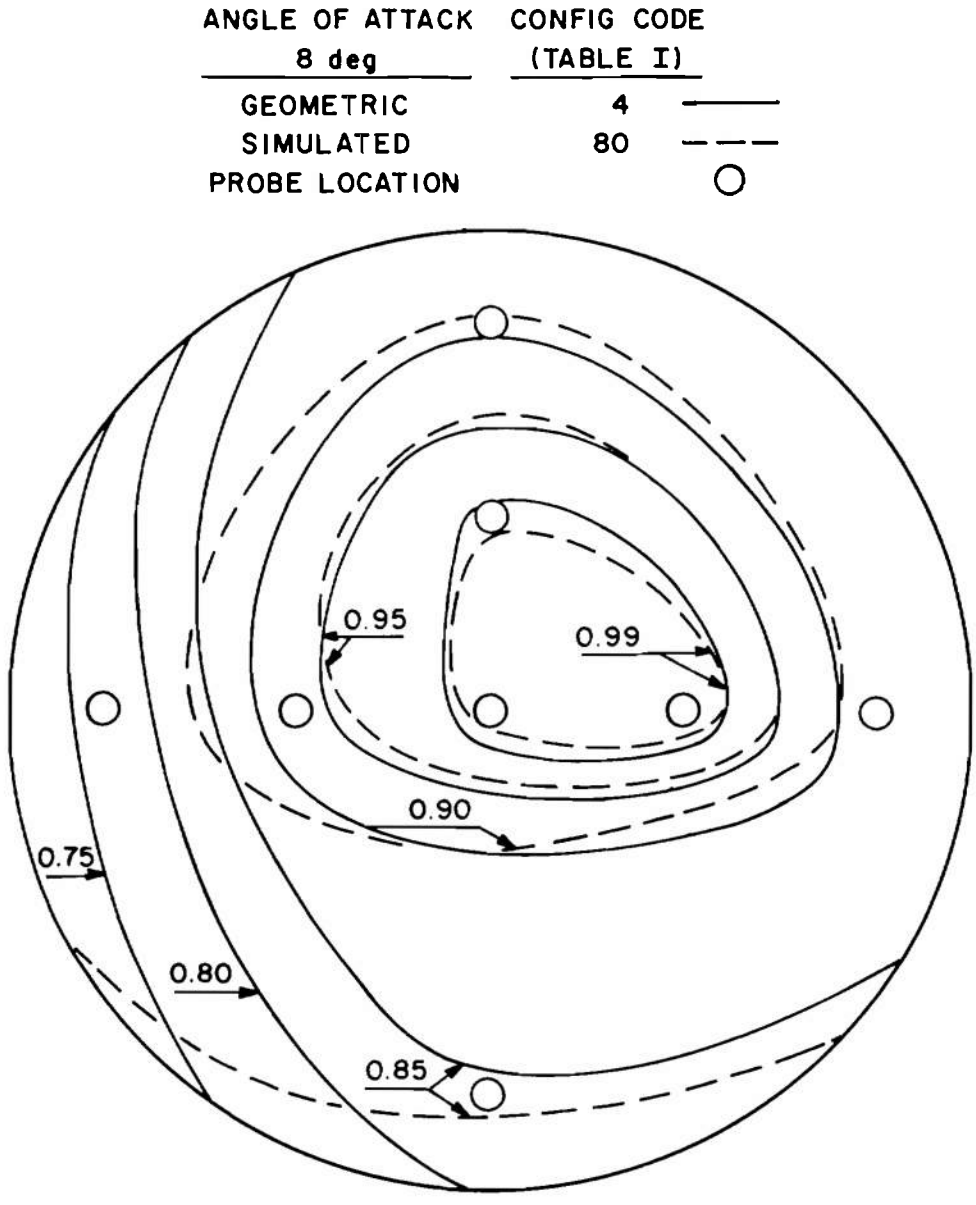

d. $M_\infty = 0.9$
Fig. 28 Continued

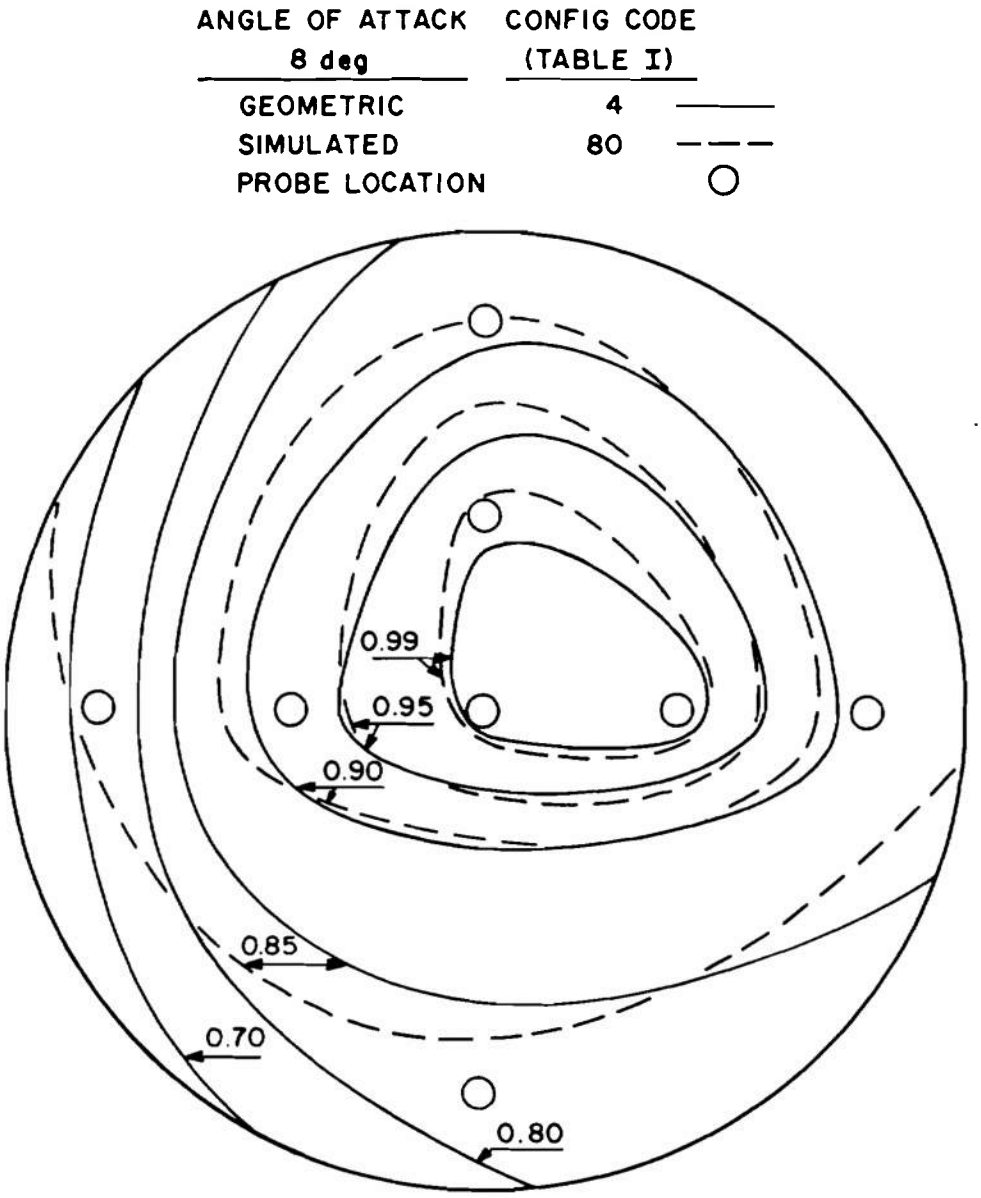

e. M_∞ = 1.0
Fig. 28 Continued

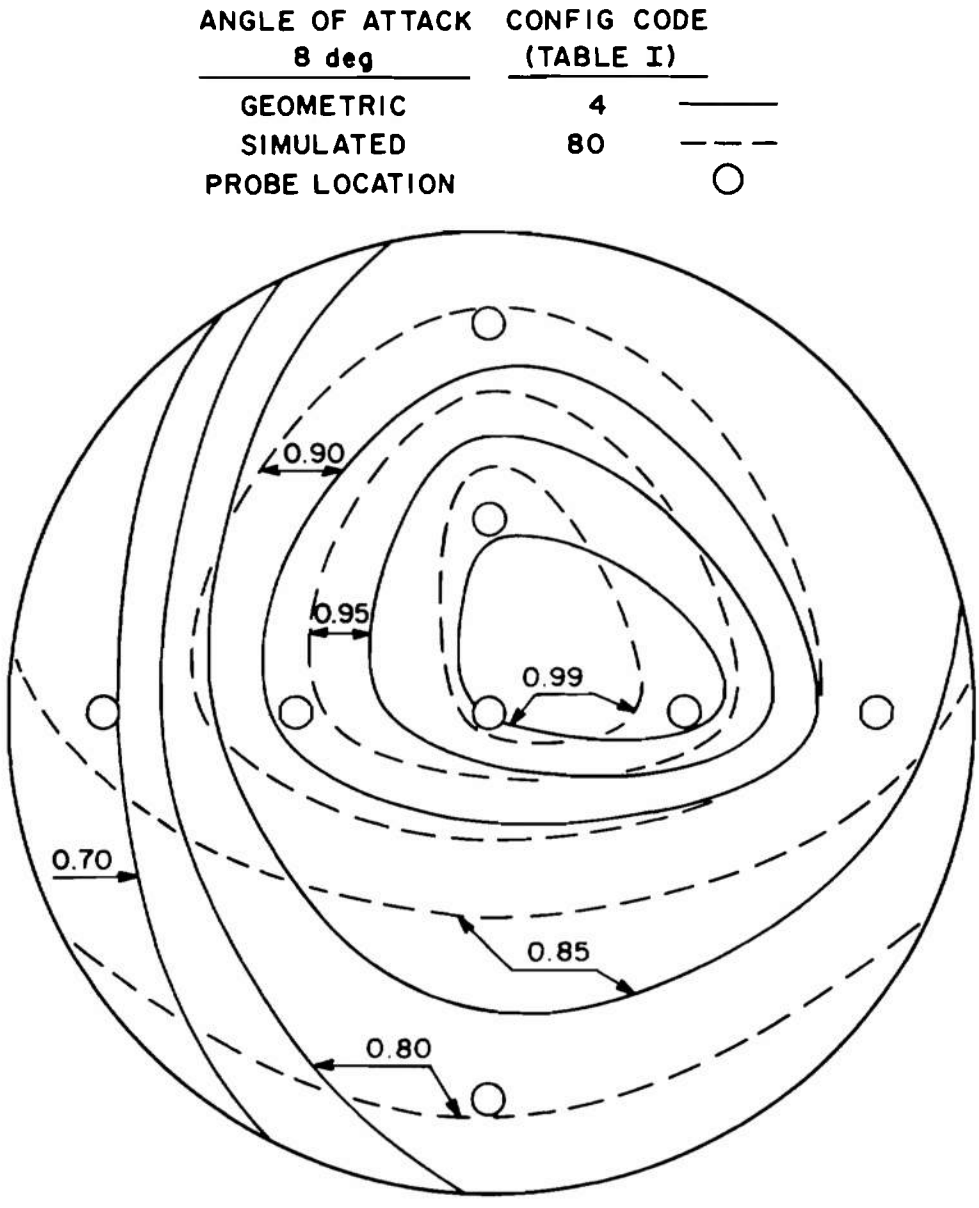

f. M_∞ = 1.1
Fig. 28 Concluded

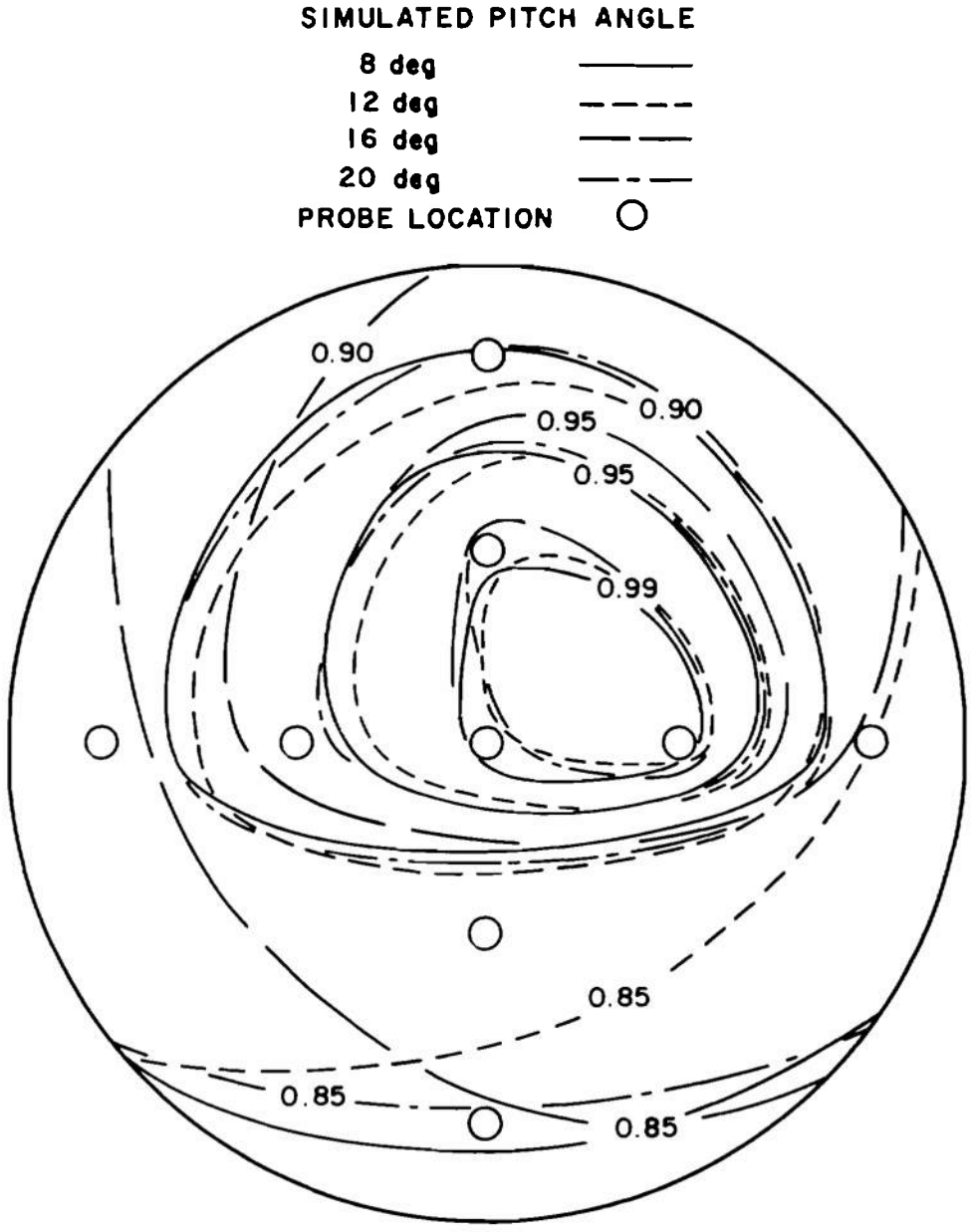

Fig. 29 Engine-Face Maps with Simulated Pitch Angle at Mach Number 0.8 ($p_{t_E}/p_{t_{E_{MAX}}}$)

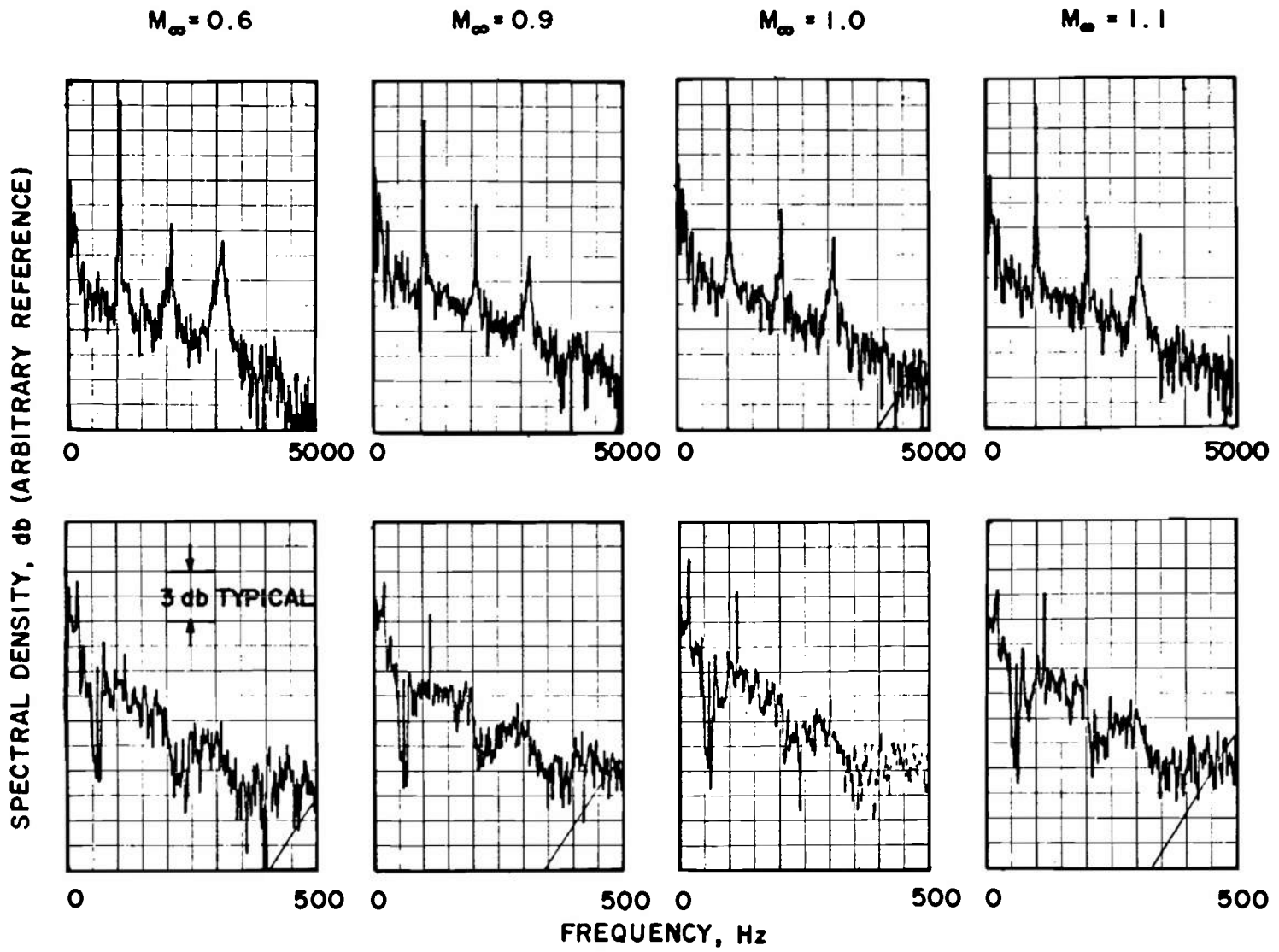

Fig. 30 Spectral Characteristics of the Test Section Total Pressure in the AEDC PWT-1T

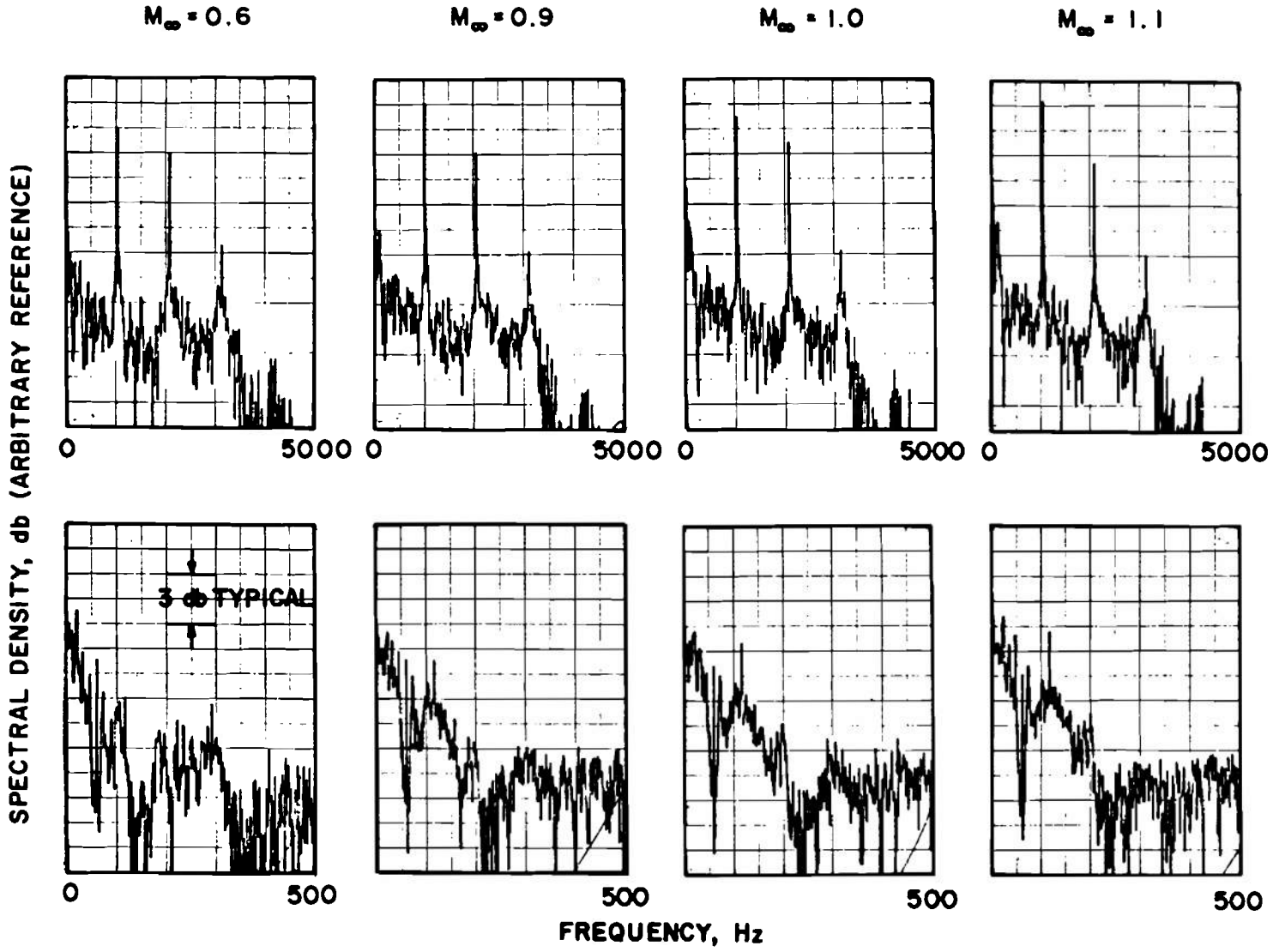

Fig. 31 Inlet Probe Spectral Data for the Basic Inlet Model at 8-deg Pitch

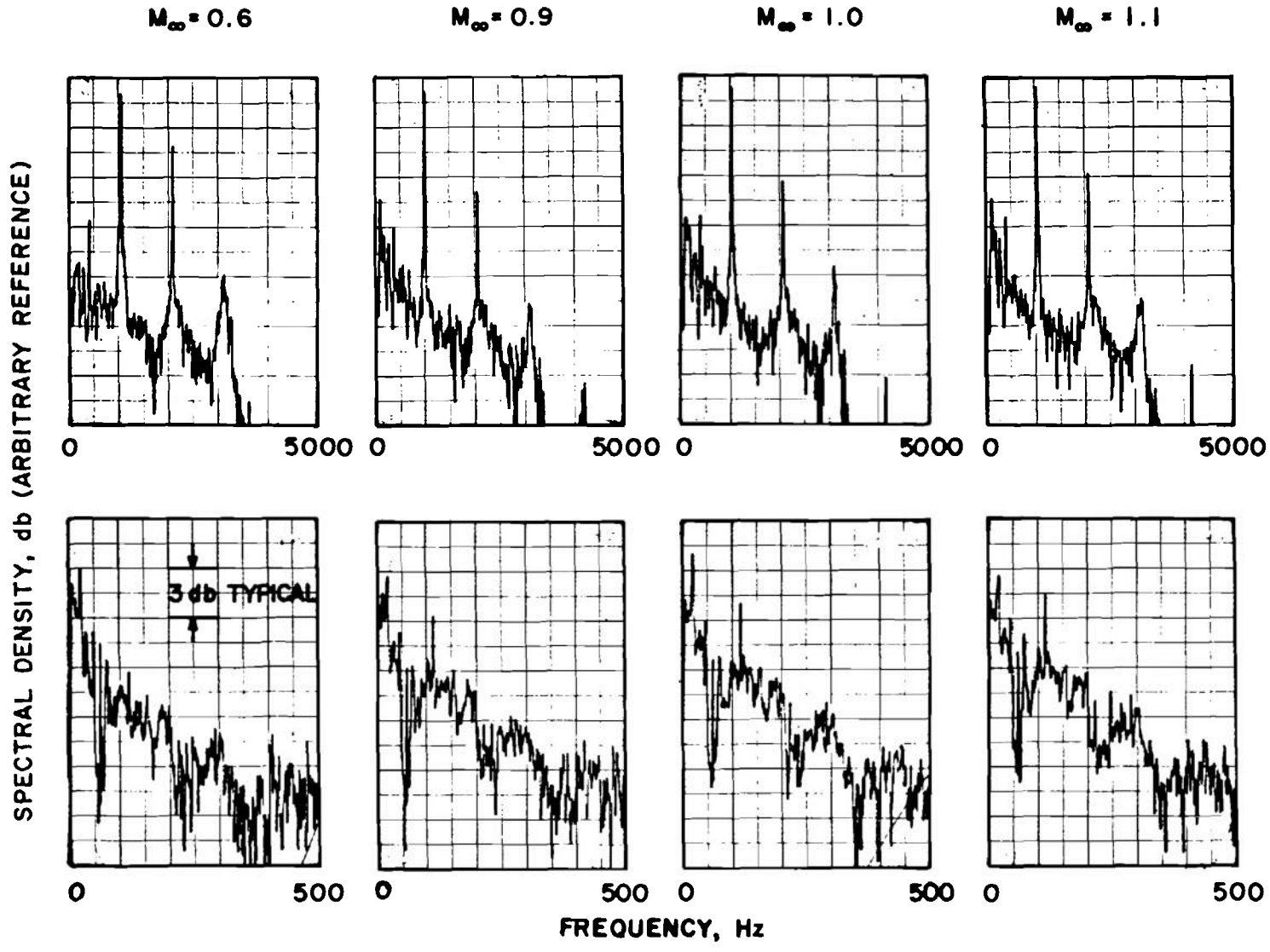

Fig. 32 Inlet Probe Spectral Data with the Inlet Model Set at 0-deg Pitch and the Modified Cylinders Set at 30-deg Pitch

TABLE I
TABULATED TUNNEL, INLET MODEL, AND MODIFIED CYLINDER SETTINGS FOR FLOW SIMULATION

Configuration Code No.	Simulated Flight		Wind Tunnel and Model Test Conditions									
								Cylinder No. 1 (Top)		Spacing	Cylinder No. 2 (Bottom)	
	Mach No.	Angle of Attack, deg	Scavenging Scoop Valve	Tunnel Wall Divergence, deg	Tunnel Free-stream Mach No.	Inlet Geometric Pitch Angle, deg	Forebody Configuration	Yaw Angle, deg	Pitch Angle, deg	Between Cylinders, in.	Pitch Angle, deg	Distance From Bottom Wall, in.
1	0.6 to 1.1	0	Open	1	0.6 to 1.1	0	N-2					
2	↓	4	↓	↓	↓	4	↓					
4		8				8						
6		12				12						
80	0.6	8			0.58	2	N-1	5	18	8.625	19	0.9
↓	0.7	↓			0.69	($\mathcal{L}$ Position)	↓	↓	19	↓	19	↓
	0.8				0.80	↓			19		19	
	0.9				0.92				18		18	
	1.0				1.03				13		13	
↓	1.1	↓			1.15				11		11	
84	0.6	12			0.55				34		34	
↓	0.7	↓			0.65				32		32	
	0.8				0.76				28		28	
	0.9				0.85				26		26	↓
74	1.0				0.96				27		23	1.25
74	1.1	↓			1.09	↓			22		20	1.25
85	0.6 to 1.1	16			Same as Config 80	10 (Std Position)			Same as Config 80		Same as Config 80	0.9
86	0.6 to 0.9	20			Same as Config 84	↓			Same as Config 84		Same as Config 84	0.9
76	1.0 to 1.1	20	↓	↓	Same as Config 74	↓	↓	↓	Same as Config 74	↓	Same as Config 74	1.25

UNCLASSIFIED

Security Classification

DOCUMENT CONTROL DATA - R & D

(Security classification of title, body of abstract and indexing annotation must be entered when the overall report is classified)

1 ORIGINATING ACTIVITY *(Corporate author)*

Arnold Engineering Development Center
Arnold Air Force Station, Tennessee 37389

2a. REPORT SECURITY CLASSIFICATION

UNCLASSIFIED

2b. GROUP

N/A

3 REPORT TITLE

EXPERIMENTAL VERIFICATION OF A TECHNIQUE FOR TESTING FULL-SCALE INLET/ ENGINE SYSTEMS AT ANGLES OF ATTACK UP TO 20 DEG AT TRANSONIC SPEEDS

4 DESCRIPTIVE NOTES *(Type of report and inclusive dates)*

Final Report - July 1, 1972 to June 30, 1973

5 AUTHOR(S) *(First name, middle initial, last name)*

R. L. Palko, ARO, Inc.

6 REPORT DATE	7a. TOTAL NO. OF PAGES	7b. NO. OF REFS
October 1973	63	5

8a. CONTRACT OR GRANT NO	9a. ORIGINATOR'S REPORT NUMBER(S)
b. PROJECT NO	AEDC-TR-73-169
c. Program Element 65802F	9b. OTHER REPORT NO(S) *(Any other numbers that may be assigned this report)*
d.	ARO-PWT-TR-73-117

10 DISTRIBUTION STATEMENT

Approved for public release; distribution unlimited.

11 SUPPLEMENTARY NOTES	12 SPONSORING MILITARY ACTIVITY
Available in DDC	Arnold Engineering Development Center, Air Force Systems Command Arnold AF Station, Tennessee 37389

13 ABSTRACT A study was conducted to demonstrate experimentally the capability of a new flow-shaping technique to extend the full-scale inlet/engine testing limit of the AEDC 16-Ft Transonic Wind Tunnel. Simulation was accomplished up to 20-deg angle of attack using a pair of modified hollow cylinder, flow-shaping devices and a 1/16-scale inlet model in the AEDC 1-Ft Transonic Wind Tunnel. This is an increase of 8 deg in pitch over the present geometric pitch limit of 12 deg. Inlet ramp and lip pressure data were used to verify the technique supported by Mach numbers measured in front of the inlet, pressures measured at the engine-face station, and inlet dynamic total-pressure data. The Mach number range covered by the study was from 0.6 to 1.1.

DD FORM 1 NOV 65 1473

UNCLASSIFIED

Security Classification

14. KEY WORDS	LINK A		LINK B		LINK C	
	ROLE	WT	ROLE	WT	ROLE	WT
verifying (experimental)						
technique						
tests						
inlet/engine systems						
angles of attack						
transonic flow						
flow-shaping devices						

AFSC
Arnold AFS Tenn